J. Biochem. **140**, 573–590 (2006)
doi:10.1093/jb/mvj186

Identification of the Positive Regulatory and Distinct Core Regions of Promoters, and Transcriptional Regulation in Three Types of Mouse Phospholipid Hydroperoxide Glutathione Peroxidase

Hirotaka Imai[1,*], Makoto Saito[1], Nozomu Kirai[1], Junya Hasegawa[1], Kumiko Konishi[1], Hiroyuki Hattori[1], Masuhiro Nishimura[2], Shinsaku Naito[2] and Yasuhito Nakagawa[1]

[1]*School of Pharmaceutical Sciences, Kitasato University, 5-9-1 Shirokane, Minato-ku, Tokyo 108-8641; and* [2]*Division of Pharmacology, Drug Safety and Metabolism, Otsuka Pharmaceutical Factory, Inc., Naruto, Tokushima 772-8601*

Received July 26, 2006; accepted August 31, 2006

Phospholipid hydroperoxide glutathione peroxidase (PHGPx) is transcribed into three types of mRNA, mitochondrial, non-mitochondrial and nucleolar types, from one gene by alternative transcription using different first exons, Ia and Ib. We investigated the regulatory mechanisms of the expressions of the three types of PHGPx using promoter analysis with luciferase as the reporter gene and electrophoretical mobility shift analysis. Here we report a draft of the positive regulatory region and the core promoter regions of PHGPx in several cell lines. From promoter deletion analysis we identified the three distinct core regions of mitochondrial PHGPx, non-mitochondrial PHGPx and nucleolar PHGPx. The core promoter activity of non-mitochondrial PHGPx was high in L929 cells, but relatively low for mitochondrial and nucleolar PHGPx. We also identified the positive regulatory region of mitochondrial PHGPx by deletion and mutation analysis of 5′-flanking regions of mitochondrial PHGPx. This region could regulate the promoter activity of non-mitochondrial PHGPx; however, up-regulation by this region was normally suppressed by the upstream region in somatic cells. Electrophoretical mobility shift analysis demonstrated that a specific transcription factor complex bound to this region in adult testis, but not in young testis and different sizes of complexes bound to this region between testis and brain.

Key words: glutathione peroxidase, positive regulatory region, promoter analysis, selenium, tissue regulation.

Abbreviations: C/EBP, CCAAT/enhancer-binding protein; CREB, cAMP responsive element binding protein; EMSA, electrophoretical mobility shift analysis; GAPDH, glyceraldehydes 3-phosphate dehydrogenase; NFY, transcription nuclear factor; PMSF, phenylmethanesulfonyl fluoride; RT, reverse transcription; RACE, rapid amplification of cDNA ends; STAT, signal transduction and activator of transcription; SP1, stimulating protein 1.

Selenium-containing glutathione peroxidases (GPx) constitute a family of anti-oxidant enzymes that are capable of reducing organic and inorganic hydroperoxides to their corresponding hydroxy compounds utilizing glutathione or other hydrogen donors as reducing equivalents (*1*). Phospholipid hydroperoxide glutathione peroxidase (PHGPx, GPx4) is a unique intracellular selenium-containing GPx that directly reduces peroxidized phospholipids that have been produced in cell membranes (*2*). Moreover, the three types of PHGPx, nucleolar, mitochondrial and non-mitochondrial types, are transcribed from one gene by alternative transcription (*3*, *4*). We have already determined that the three types of PHGPx play several independent and important roles in the modulation of inflammation, spermatogenesis and cell death by using three types of PHGPx overexpressing cells (*5*–*11*). Non-mitochondrial PHGPx suppressed the activation of lipoxygenase and cyclooxygenase at the nucleus and endoplasmic reticulum in response to several stimuli (*5*, *6*), although it did not suppress apoptotic cell death induced by the mitochondrial death pathway (*9*). On the other hand, mitochondrial PHGPx can suppress the release of cyt.*c* from mitochondria during apoptosis induced by the mitochondrial death pathway, although it cannot suppress the activation of lipoxygenase and cyclooxygenase (*5*, *6*, *8*, *9*). Non-mitochondrial PHGPx also suppress the production of platelet activating factor by stimulation with A23187 (*7*), while nucleolar PHGPx suppresses cell death induced by nucleolar damage (*10*). Thus, the three types of PHGPx distributed in different organelles play different roles in signal transduction, inflammation, and apoptosis. However, details of the regulatory mechanisms of the expressions of the three types of PHGPx in various tissues are unknown.

We previously cloned the gene for mouse PHGPx and created PHGPx knockout mice (*3*). Recently, the complete genomic sequences of the human, pig and mouse have become available (*12*–*14*). Computer analysis of the 5′-flanking regions of PHGPx have shown evidence of conserved consensus binding sequences for several transcription factors; however, except for the core promoter region, the functionalities of these binding motifs have not been

*To whom correspondence should be addressed. Tel: +81-3-5791-6236, Fax: +81-3-5791-6236, E-mail: imaih@pharm.kitasato-u.ac.jp

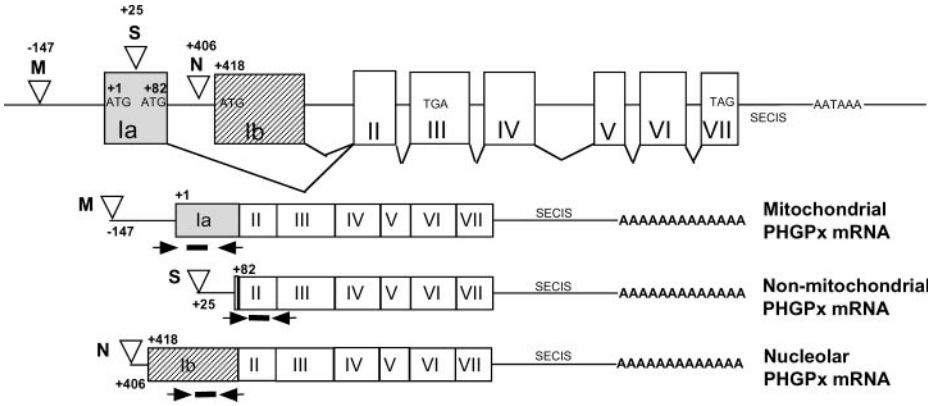

Fig. 1. **Structure of the PHGPx gene, three types of PHGPx mRNAs and the primer sets for TaqMan RT-PCR.** The structure of the mouse PHGPx gene (Accession No. AB030643) includes eight exons in the upper panel, while those of the three types of PHGPx mRNA are shown in the under panel. The exon Ia (gray box) includes the translational first start site ATG (+1) for mitochondrial PHGPx, and the second ATG (+82) for non-mitochondrial PHGPx. The exon Ib (shadow box) includes the translational third start site ATG (+418) for nucleolar PHGPx. The reverted open triangles show three transcriptional start sites by analysis of 5′ RACE as previously reported; position −147 is the transcriptional start site for mitochondrial PHGPx (M), position +25 for non-mitochondrial PHGPx (S) and position +406 for nucleolar PHGPx (N). TGA in exon III encodes selenocysteine, the active site; and TAG in exon VII encodes the stop codon. SECIS is the selenocysteine insertion sequence. Arrowheads indicate the TaqMan RT-PCR primers used for detection of the three types of PHGPx and black bars indicate the TaqMan probe.

studied in detail (*15*, *16*). PHGPx genomic DNA consists of eight exons encoding mitochondrial, non-mitochondrial and nucleolar PHGPx (Fig. 1). Analysis of 5′ RACE showed that there were three independent translational start sites for the three types of PHGPx and promoter regions in the PHGPx gene. The first translational start codon for mitochondrial PHGPx and the second translational start codon for non-mitochondrial PHGPx are in the first exon, Ia, of PHGPx genomic DNA, with a mitochondrial targeting signal existing between the first and second translational start codon (*17*). The third translational start codon for 34 kDa nucleolar PHGPx exists in exon Ib (*10*, *18*). On the other hand, transcriptional start sites exist in the upstream of each translational start codon, as shown in Fig. 1 and reported previously (*4*, *10*, *19*). Transcriptional regulation of the PHGPx gene is highly complex since three different proteins can be synthesized from one gene, and the transcriptional start site for non-mitochondrial PHGPx exists within exon 1a including the coding region for mitochondrial PHGPx. It is unclear whether the synthesis of the two mitochondrial and non-mitochondrial PHGPx isoforms is regulated by a uniform mechanism or whether their expression is under the control of different *cis*-regulatory elements.

The three isoforms of PHGPx show remarkable tissue-specific expression patterns (*11*, *20*, *21*). Non-mitochondrial PHGPx are widely expressed in most cultured cells and tissues tested, but are much more prominent in testis by Northern blot analysis (*20*, *21*). Expression of mitochondrial PHGPx is expressed at low levels in somatic cells and is induced during spermatogenesis in testis (*11*, *20*, *22*). Expression of nucleolar PHGPx was first detected only in testis (*18*), but we found that nucleolar PHGPx is widely expressed in various rat tissues at extremely low levels (*10*). Especially mitochondrial PHGPx has an important role in spermatogenesis and sperm function, and its deficiency is implicated in human infertility (*11*, *22–24*). Thus, the mechanism of the high expression of mitochondrial PHGPx in testis or the repression of the expression of mitochondrial PHGPx in somatic cells can be linked when attempting to clarify infertility in patients. Unfortunately, the regulatory mechanisms involved in this repression in somatic tissues and in the high-level expression of the enzyme in germinative cells are essentially unknown. The lack of experimental data on the regulation of the expressions of the three types of PHGPx gene and their remarkable tissue-specific expression patterns prompted us to study the regulatory mechanisms involved in PHGPx expression, and to identify the positive or negative regulatory regions of the three types of PHGPx.

In this study we found the positive regulatory regions and the core regions of the three types of PHGPx by deletion and mutation analysis of their promoter regions in somatic cells. The positive regulatory region in the promoter region of mitochondrial PHGPx, which contains a novel transcriptional factor binding sequence, could regulate the promoter activity of non-mitochondrial PHGPx; but in somatic cells this activity is repressed by the upstream region. Electrophoretical mobility shift analysis indicated that different sizes of complexes bound to this region between testis and brain, and a specific transcription factor complex bound to this region in adult testis, but not in young testis.

MATERIALS AND METHODS

Cell Culture Conditions—Mouse fibrosarcoma L929, mouse Y1 cells and human HeLa cells were maintained in Dulbecco's modified Eagle's medium supplemented with 5% (v/v) fetal calf serum and the antibiotics 100 units/ml penicillin and 100 μg/ml streptomycin at 37°C under 5% CO_2. TT2 embryonic stem cells (ES cells) were maintained in Dulbecco's modified Eagle's medium supplemented with 20% (v/v) fetal calf serum, 1% (v/v) Non-essential amino acids solution (GIBCO), 1 mM Sodium pyruvate, 0.001% (v/v) 2-Mercaptoethanol and 300 unit Leukemia inhibitory factor (LIF; CHEMICON).

Isolation of RNA—Total RNA was isolated from adult mice tissues and cultured cells using Isogen (Nippon Gene Co. Ltd., Tokyo, Japan) according to the manufacturer's instructions. RNA was quantified by optical density and stored at –80°C

Experimental Conditions for TaqMan RT-PCR—The total RNAs obtained from adult mice tissues and cultured cell lines were diluted with RNase-free water to 20 μg/ml, then further diluted with 50 μg/ml yeast tRNA. To prepare the calibration curve, various amounts of total RNA ranging from 6.4 to 100,000 pg were used. For the RT-PCR reaction, a TaqMan One-Step RT-PCR Master Mix Reagents Kit (Applied Biosystems) containing 300 nM forward primer, 900 nM reverse primer, and 200 nM TaqMan probe was used at 50 μl/tube. For specific detection of mitochondrial PHGPx mRNA in various tissues, we used the following primer sets; forward primer, 5′-AGCTGGGGCCGTCTGAGCCG-3′, reverse primer, 5′-ATGTCCTTGGCTGAGAATTCGT-3′, TaqMan probe, 5′-CCTGGTCTGGCAGGCACCATGTGT-3′. For specific detection of nucleolar PHGPx mRNA in various tissues, we used the following primer sets; forward primer, 5′-CTGAACCTTTCAACCCGGG-3′, reverse primer, 5′-AGAATTCGTGCATGGAGCG-3′, TaqMan probe, 5′-TCTGCTGCAAGAGCCTCCCCAGTACT-3′. For detection of total PHGPx mRNA (non-mitochondrial, mitochondrial and nucleolar PHGPx) in various tissues, we used the following primer sets; forward primer, 5′-CGCGATGATTGGCGCT-3′, reverse primer, 5′-CACACGAAACCCCTGTACTTATCC-3′, TaqMan probe, 5′-TCCATGCACGAATTCTCAGCCAAGGA-3′. For calculating the relative expressions of PHGPx mRNA, we used the following mouse glyceraldehydes-3-phosphate dehydrogenase (GAPDH) primer sets; forward primer, 5′-TGCAGTGGCAAAGTGGAGAT-3′, reverse primer, 5′-TGCCGTGAGTGGAGTCATACT-3′, TaqMan probe, 5′-CCATCAACGACCCCTTCATTGACCTC-3′.

Statistical Analysis for TaqMan RT-PCR—Samples were deemed positive at any given cycle when the value of the emitted fluorescence was greater than the threshold value calculated by the instrument's software (Sequence Detector Ver. 1.9.1). The threshold cycle (C_t), which is defined as the cycle at which PCR amplification reaches a significant value (*i.e.*, usually 15 times greater than the standard deviation of the baseline), is given as the mean value. The source of total RNA for the measurement of calibration data was mouse adult testis. The relative expression of each mRNA was calculated by the ΔC_t method (where ΔC_t is the value obtained by subtracting the Ct value of the GAPDH mRNA from the C_t value of the target mRNA, as employed in our earlier studies (*25*). Specifically, the amount of target relative to the GAPDH mRNA was expressed as $2^{(\Delta Ct)}$. Data are expressed as the ratio of target mRNA to GAPDH mRNA. Studies were conducted in triplicate and data are shown as mean ± SD of three runs.

Construction of Chimeric Plasmids—The *Kpn*I genomic PCR fragment corresponding to the 5′ flanking region of the three types of PHGPx; the promoter region from –1427 to +39 bp for non-mitochondrial and mitochondrial PHGPx (S1), the promoter region from –1427 to –146 for mitochondrial PHGPx (M1) and the promoter region from +84 to +401 for nucleolar PHGPx (N1) were subcloned into the *Kpn*I site of the pGL3-Basic vector (Promega, Madison, WT). For amplifying the promoter region (–1427/+39) of non-mitochondrial and mitochondrial PHGPx, we used the PHGPx genomic DNA we previously cloned (*3*) as a template and the following primer sets; forward primer, 5′-ATTGGTACCGCTGAGCTGAGGAATGTCC-3′ and reverse primer, 5′-TAGGGTACCAGATCTTGCTGGCTTAAGTAAGCGG-3′. For amplify the promoter region (–1427/–146) of mitochondrial PHGPx, we used the following primer sets; forward primer, 5′-ATTGGTACCGCTGAGCTGAGGAATGTCC-3′, and reverse primer, 5′-TTAGGTACCAGATCTCAGCCAATGGGAAGCCTGA-3′. For amplifying the promoter region (+84/+401) of nucleolar PHGPx, we used the following primer sets; forward primer, 5′-ATTGGTACCGTGGGCTACTGGGAACTTG-3′, and reverse primer, 5′-ATTGGTACCAGATCTTTGTTCAACCCCGGAGATG-3′. To generate 5′ stepwise and 3′ stepwise deletion constructs, PCR procedures were performed using sets of primers specific for the PHGPx sequence, and S1 plasmid, pGL3 (–1427/+39), the M1 plasmid, pGL3 (–1427/–146) and the N1 plasmid, pGL3 (+84/+401) as templates. These PCR products were subcloned into the pTZ18R vector, followed by digestion with *Kpn*I, and subcloned into the *Kpn*I site of the pGL3-Basic vector.

5′ stepwise deletion and substitution mutation constructs for identification of the positive regulatory region were generated by PCR amplification using the M5 plasmid, pGL3 (–358/–146) as a template. For construction of substitution mutation plasmids M13–M18, we used the forward primer M13; 5′-ATTGGTACCTCCGAGAGGTTCCCCAAAGCGC-3′, M14; 5′-ATTGGTACCTCCCAGGGGTTCCCCAAAGCGC-3′, M15; 5′-ATTGGTACCTCCCAGAGGGTCCCCAAAGCGCCCTGGC-3′, M16; 5′-ATTGGTACCTCCCAGAGGTTCTTTAAAGCGCCCTGGCACCCT-3′, M17; 5′-ATTGGTACCTCCCAGAGGTTCCGCAAAGCGCCCTGGCACCCT-3′, M18; 5′-ATTGGTACCTCCCAGAGGTTCCCCAAATCGCCCTGGCACCCT-3′ and the reverse primer, 5′-TTAGGTACCAGATCTCAGCCAATGGGAAGCCTGA-3′. PCR products were digested with *Kpn*I and subcloned into the *Kpn*I site of the pGL3-Basic vector.

Vectors with a mutation at the NFY binding sequence in the H11, H12 homology domain, the AP2 binding sequence in the H13 homology domain, the SP1 binding sequence in the H26 homology domain or the CREB binding sequence in the H27 homology domain were constructed with QuickChange Site-Directed Mutagenesis Kit (Stratagene, TX, USA), and DNA sequences of mutated vectors were confirmed by sequence analysis. The sequences of the mutation site (underlined) of the vector are as follows: Mutant NFY in H11 domain of M9, S13 and S16 vectors: 5′-TCATTCAGGCTTCCCAACTTG-TGCAGGGGCCTCGCG-3′; Mutant NFY in H12 domain of S14 and S17 vectors: 5′-CGCAGGCGCATCTGATCGATAAGAGACGTCAGT-3′; Mutant AP2 in H13 domain of S15 and S16 vectors: 5′-GACGTCAGTGGGCGTTTTTGAGGGCGGGCAAGCC-3′; Mutant SP1 in H26 domain of N8 vector: 5′-TGGTCACGCGCCCTGAAAGGCC-TGGTGCGTCACA-3′; Mutant CREB in H27 domain of N9 vector: 5′-CCTGCCCGGCCTGGTGGCTAGCAGTCGGCGGCGCCTTG-3′. The sequences of the wild type in these several domains are listed in Table 3.

Transient Transfection and Luciferase Assay—Transient transfection experiments were carried out using L929, Y1

and HeLa cells placed at a density of 6×10^4 per 24 well dish approximately 18 h before transfection. For transient transfection, 400 ng of plasmid DNA was transfected into these cells using the LipofectAMINE Plus reagent system (Invitrogen). Plasmid pRL-SV40 vector (Promega) was always cotransfected as an internal control for transfection efficiency. After an additional cultivation for 24 h, the transfected cells were harvested, lysed, centrifuged to pellet the debris and subjected to luciferase assay. Luciferase activities were measured as chemiluminescence in liquid scintillation and luminescence counters, 1450 MicroBeta, TRILUX (WALLAC), using the Dual-luciferase Reporter Assay System (Promega) according to the manufacture's protocol. All transfections were repeated in triplicate. The activity of firefly luciferase was normalized to that of Renilla luciferase. Data represent fold activations of each luciferase activity against the luciferase activity of the promoterless pGL3-Basic vector (Promega) from three independent experiments.

Preparation of Nuclear Extracts from Mouse Tissues and Cells—Mice (BALB/c, 6 weeks old and 2 weeks old) were sacrificed by diethyl ether inhalation and brain and testis were prepared. The organs were homogenized in a glass Dounce homogenizer (loose type) in ice-cold Phosphate Buffered Saline (PBS), centrifuged at 2,000 rpm for 5 min at 4°C, and washed with ice-cold PBS. 1×10^8 L929 cells and TT2 embryonic cells were scraped in ice-cold PBS, centrifuged for 5 min at 1,000 rpm, and washed with PBS before being centrifuged again. For nuclear extracts, the homogenized organs and collected cultured cells were lysed in 20 mM HEPES buffer, pH 7.9, containing 5 mM KCl, 0.5 mM $MgCl_2$, 0.5 mM DTT, and 0.5 mM PMSF. After 10 min on ice the cells were homogenized in a glass Dounce homogenizer (tight type) and centrifuged again at 2,000 rpm for 5 min at 4°C. The nuclear pellet was resuspended in 20 mM HEPES buffer, pH 7.9, containing 25% glycerol, 300 mM NaCl, 0.5 mM $MgCl_2$, 0.2 mM EDTA, 0.5 mM DTT, and the proteinase inhibitor mixture and was then mixed by rotation at 4°C for 1 h. The suspension was centrifuged at $10,000 \times g$ for 30 min at 4°C and dialyzed twice with 20 mM HEPES buffer, pH 7.9, containing 50 mM KCl, 0.5 mM EDTA, 10% Glycerol, 0.5 mM DTT, and 0.5 mM PMSF. The suspension was centrifuged at $10,000 \times g$ for 30 min at 4°C and the supernatant stored at –80°C. The protein concentration of the nuclear extracts was determined by Bradford assay (Bio-Rad, Hercules, CA) using bovine serum albumin as a standard.

Electrophoretical Mobility Shift Analysis (EMSA)—The wild-type and mutant probes used for EMSA assay are listed in Table 4. Double-strand oligonucleotide probes were generated by annealing equimolar complementary oligonucleotides. All probes were radiolabeled with [γ-^{32}P]ATP using a MEGALABEL DNA 5′-End labeling Kit (TAKARA, Co. Ltd.). Binding reactions were carried out for 30 min at 4°C in 25 μl of binding buffer (100 mM HEPES, pH 7.9, 250 mM KCl, 5 mM EDTA, 25 mM DTT, 2 mg/ml BSA) containing 10–20,000 cpm of labeled probe, 1 μg of poly(dI-dC), and 5 μg of nuclear extracts. For competition assays, double-strand oligonucleotides containing a consensus STAT (STAT-c; in Table 4), a STAT mutant binding site (STAT-m; in Table 4), a wild-type H3 homology domain (f; in Table 4), a H3 homology domain mutant (fm1-5; in Table 4) a consensus NFY (NFY-c, in Table 4), a consensus AP2 (AP2-c; in Table 4), a consensus SP-1 (SP1-c, in Table 4), a H10, H11 homology domain (k, in Table 4) and a H26 homology domain (x, in Table 4) were generated by annealing equimolar complementary oligonucleotides. For supershift assay, anti-SP1, anti-AP2, anti-NFY, anti-C/EBPβ, anti-CREB1, anti-GATA1, anti-GATA4, anti-STAT1, anti-STAT3 and anti-STAT4 polyclonal antibodies (Santa Cruz Biotechnology, Santa Cruz, CA) were purchased. For these interference assays, 50–100 fold molar excesses of unlabeled competitor or 4 μg of antibody were added to the reaction mixtures for 1 h at 4°C before the addition of a radiolabeled probe. The DNA-protein complexes were separated on a 6% non-denaturing polyacrylamide gel in a 0.25× Tris acetic acid electrophoresis buffer at 200 V. Following completion of the running, the gel was transferred onto 3MM paper and dried under vacuum. The dried gel was then visualized by autoradiography using a Bio Imaging Analyzer BAS-2000II (FUJIX).

RESULTS

Tissue Distributions of the Three Types of PHGPx in Mice and Cultured Cells—The three types of PHGPx, non-mitochondrial PHGPx, mitochondrial PHGPx and nucleolar PHGPx, are transcribed by alternative transcriptions from one gene (Fig. 1). Initially, we developed TaqMan real time PCR methods to quantify the amounts of the three types of PHGPx mRNA and compared the levels of the expressions of the three types of PHGPx in various tissues of BALB/c mice and culture cells. Nucleolar PHGPx and mitochondrial PHGPx could be specifically detected by specific primer sets and the TaqMan probe because they are transcribed from exon Ia and exon Ib, respectively (Fig. 1). On the other hand, mRNA for non-mitochondrial PHGPx could not be differentiated from mitochondrial PHGPx, since mRNA for non-mitochondrial PHGPx are transcribed from half of exon Ia and has the same sequences as that of the 3′ part of mitochondrial PHGPx mRNA. We detected it as total PHGPx using primers from Exon II and III by TaqMan real time-PCR in Fig. 1, and Tables 1 and 2. GAPDH was used as the endogenous

Table 1. **Calibration data and limit of quantification for each mRNA in the total RNA studied.**

mRNA	No. of data points	Calibration curve		Correlation coefficient (r)	Limit of quantification (pg total RNA/50 μl reaction mixture)
		Slope	Intercept		
Mitochondrial PHGPx	7	–3.35	33.06	1.00	6.4
Total PHGPx	7	–3.31	32.14	1.00	6.4
Nucleolar PHGPx	5	–3.85	38.53	1.00	160

The calibration curves show the threshold cycle (C_t) for analysis of total RNA per 50 ml of reaction mixture. The source of total RNA was the mouse testis.

Table 2. **Expression for three types of PHGPx mRNA in mouse various tissues and cultured cells.**

Tissue	Total PHGPx	Mitochondrial PHGPx	Nucleolar PHGPx
Liver	0.547 ± 0.152	0.0622 ± 0.00913	0.000251 ± 0.0000222
Kidney	0.802 ± 0.147	0.0657 ± 0.0143	0.000444 ± 0.0000876
Heart	0.406 ± 0.0680	0.0656 ± 0.0221	0.000636 ± 0.000599
Brain	0.313 ± 0.0479	0.138 ± 0.0140	0.000241 ± 0.000181
Lung	0.896 ± 0.364	0.174 ± 0.119	0.000789 ± 0.000280
Testis	22.4 ± 9.88	22.1 ± 10.17	1.56 ± 0.642
Spleen	0.431 ± 0.118	0.114 ± 0.0540	0.0000648 ± 0.00000997
Intestine	0.620 ± 0.173	0.0800 ± 0.0321	0.0000770 ± 0.0000343
Uterus	0.841 ± 0.444	0.101 ± 0.0318	0.0000935 ± 0.0000246
Ovary	0.666 ± 0.142	0.115 ± 0.0457	0.000317 ± 0.000170
L929	0.471 ± 0.0900	0.0124 ± 0.00319	0.000102 ± 0.0000237
MEF	0.427 ± 0.0467	0.0316 ± 0.00169	0.000255 ± 0.0000396

Data are expressed as the ratio of target mRNA to GAPDH mRNA. Experiments were performed in triplicate, and data are shown as the mean ± SD of three runs. MEF, mouse embryonic fibroblast.

control in the measurement of the three types of PHGPx mRNAs. PCR products were amplified as single bands respectively by reverse and forward primers and verified by nucleotide sequence to confirm the specificity of the amplified PHGPx cDNA (data not shown). Table 1 shows the calibration data and the limit of quantification for each mRNA in the total RNA studied. The source of total RNA was derived from a pool of adult mouse testis samples. The lower limit of quantification of each of the mRNAs ranged from 6.4 to 160 pg of total RNA per 50 ml of reaction mixture. Table 2 shows the ratio of PHGPx mRNA to GAPDH in several tissues of mouse, mouse embryonic fibroblast and mouse fibroblast L929 cells. Mitochondrial PHGPx, nucleolar PHGPx and total PHGPx showed the highest level of mRNA expression in mouse testis. The amounts of total mitochondrial and nucleolar PHGPx mRNA in testis were about 25–71, 127–133 and 1,668–6,500 times higher than that in somatic tissues such as liver, kidney and brain. In somatic tissues and cultures cells, the amounts of total PHGPx mRNA were about 2.26–12.2, 638–8,994 times higher than that of mitochondrial and nucleolar PHGPx mRNAs. These results indicated that the expression of non-mitochondrial PHGPx was relatively high in somatic cells while the expression of nucleolar PHGPx was extremely low. On the other hand, the expression of mitochondrial PHGPx and nucleolar PHGPx were significantly high in only testis.

Comparison of Promoter Activities of the Three Types of PHGPx in Somatic Cells—The PHGPx gene encoding for pig (*12*), human (*13*), and mouse (*3*, *14*) have recently been cloned and sequenced by several groups, including international genomic sequence projects and ours (*3*; Accession No. AB030643). 5′ RACE method analysis in a previous report showed that the transcriptional start site for mitochondrial PHGPx existed at –147 bp in the upstream of exon 1a (Fig. 2A), if the first ATG for mitochondrial PHGPx in exon Ia is position +1 (*19*). On the other hand, our previous analysis showed that the transcriptional start site for non-mitochondrial PHGPx mainly existed at +25 bp within exon Ia (Accession No.AB030643). The transcriptional start site for nucleolar PHGPx existed at +406 bp in the upstream of exon Ib, as reported by our 5′ RACE method (*10*, *21*). This evidence and the expression data suggested that there are three distinct core promoter regions and regulatory regions. By comparison of sequences in the 5′-flanking regions of pig, human and mouse, we determined 29 high homology domains (H1 to H29) as shown by the gray and black circles in Fig. 2A and Table 3. Using computer analysis (http://transfac.gbf.de/TRANSFAC/), we identified that twelve regions of the 29 homology domains contained the putative consensus binding sequences for several transcriptional factors in Table 3. However, 17 regions of these homology domains did not contain putative transcriptional factor binding sequences. These homology domains with or without putative transcriptional factor binding sites are shown in black or gray circles (Fig. 2A).

We first examined the promoter activities of the three types of PHGPx. We made constructs of the three basic reporter gene vectors (S1, M1, N1) that include each 5′-flanking region before the transcriptional start sites of the three types of PHGPx (Fig. 2B). Luciferase vector M1 can be measured by the promoter activity of mitochondrial PHGPx, and luciferase vector N1 can be measured by the promoter activity of nucleolar PHGPx. On the other hand, the 5′-flanking region (–1427 to +39) for non-mitochondrial PHGPx is more complex, since the 5′-flanking region (–1427 to +39) includes two core promoter regions, two transcriptional start sites of both mitochondrial and non-mitochondrial PHGPx, and one translational start site of mitochondrial PHGPx. To measure only the promoter activity of non-mitochondrial PHGPx, we made a construct of a series of luciferase vector S by insertion of a 5′-flanking region (–1427 to +39) to the pGL3 luciferase reporter gene vector (Fig. 2C). Even if mitochondrial types of luciferase mRNA are transcripted from the first transcriptional start site (M) by using the promoter activity for mitochondrial PHGPx, followed by translation of mitochondrial type of luciferase product from the first start codon (+1), the translation products are stopped in termination codon TAA (+97 to +99) that exist before the translation start site (+133) of intact luciferase protein. Therefore, the luciferase vector S series can be measured by just the promoter activity of non-mitochondrial PHGPx, without the effect of the promoter activity of mitochondrial PHGPx.

To compare the promoter activity of the three types of PHGPx, a series of chimeric luciferase vectors (S1, S7, M1 and N1) were transfected into several kinds of cell lines such as mouse L929 (Fig. 2D), mouse Y1 (Fig. 2E) and

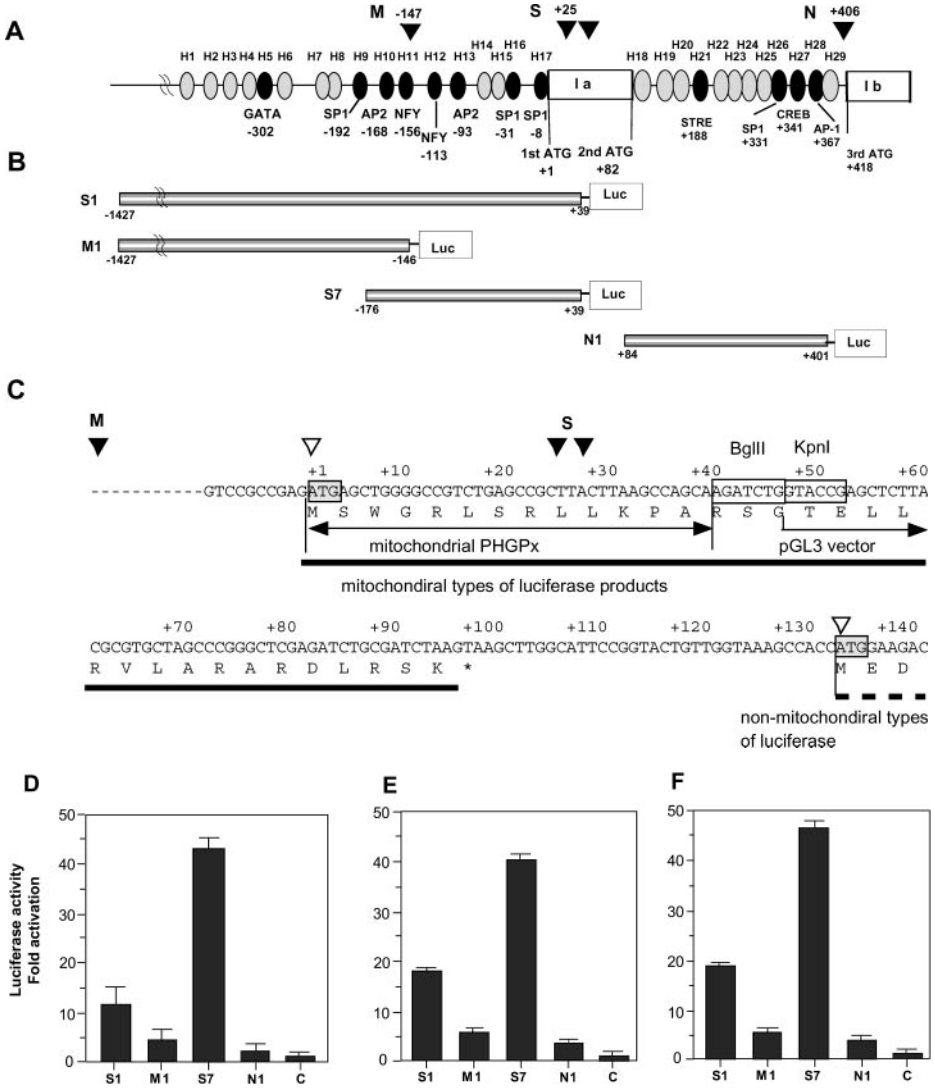

Fig. 2. **Functional promoter activities of three distinct types of PHGPx.** (A) Putative transcriptional factor binding sites and homology domains of the 5′-flanking region of exon Ia and exon Ib of the PHGPx gene. The gray and black circles represent the homology domains (H) of the 5′-flanking region of exon Ia and exon Ib between human, pig and mouse as indicated in Table 3. The number of homology domains (H) is shown in Table 3. The black and gray circles are homology domains with and without putative transcriptional factor binding sites by analysis of the TRANSFAC program. Black inverted triangles indicated the transcriptional start sites of the three types of PHGPx; mitochondrial PHGPx (M), non-mitochondrial PHGPx (S) and nucleolar PHGPx (N), as identified by 5′ RACE analysis. (B) Construction of reporter gene vectors of the three types of PHGPx. S1 includes the promoter region of both mitochondrial PHGPx and non-mitochondrial PHGPx. M1 includes the promoter region of the 5′-flanking regions of mitochondrial PHGPx. S7 includes only the promoter regions of the 5′-flanking regions of non-mitochondrial PHGPx. N1 includes the promoter region of nucleolar PHGPx. The number indicates the gene base pair of PCR fragments of the 5′-flanking regions used for reporter gene construction. (C) Design of luciferase vector (S) to measure only promoter activity for non-mitochondrial PHGPx. S1 and S7 luciferase vectors contain two transcriptional start sites of mitochondrial PHGPx (M; reverted closed triangle) and non-mitochondrial PHGPx (S; reverted closed triangles). The 5′-flanking region of the promoter of non-mitochondrial PHGPx is inserted to the *Kpn*I restriction enzyme site in the pGL3 luciferase vector. If translation is started from the translational start site of mitochondrial PHGPx (+1; first open reverted triangle), mitochondrial types of luciferase products (under line) are stopped at stop codon TAA (+97) in the pGL3 vector. If transcription is started from the start site of non-mitochondrial PHGPx (S; reverted closed triangles), translations for non-mitochondrial types of luciferase are started from the start codon (+133; second open reverted triangle) of firefly luciferase in the pGL3 vector (dot line). (D–F) Relative luciferase activity of the different promoter constructs of the three types of PHGPx in several cell lines; L929 (D) Y1 (E) and HeLa (F). Cells were transfected with the firefly luciferase constructs connected with the different promoters of the three types of PHGPx using a lipofectoamine plus transfection kit. To correct luciferase activity measured for transfection efficiency, cotransfections with a control renilla luciferase plasmid were carried out. The relative luciferase activity of the negative control (C; pGL3 basic vector) is indicated as 1.0.

human HeLa (Fig. 2F) cells, and luciferase assays carried out. The strongest relative activity of luciferase was indicated by luciferase vector S7 (–176/+39). The activities of luciferase from vectors M1 and N1 were significantly lower compared with that of luciferase vector S7. The longest construct, S1 (–1427/+39), derived from a 1.4 kb genomic fragment of the 5′-franking region of non-mitochondrial PHGPx had half or a third of the activity of that of

Table 3. **Identification of homology domains in 5′-flanking regions of exon Ia and Ib in PHGPx gene between mouse, pig and human.**

Homology domain number	Homology region gene base number	The number of identical nucleic acids		Predicted transcription factor binding site	Sequences
		human/mouse	pig/mouse		
H1	–445 -------- –437	9/9	6/9		TAGCCTGG
H2	–377 -------- –360	13/18	9/18		GACTTTGACACGCTTTTCT
H3	–354 -------- –344	7/11	9/11		CAGAGGTTCCC
H4	–321 -------- –308	12/14	11/14		CGCTGCAGGCAACC
H5	–304 -------- –296	10/10	9/10	GATA	CGGATAACTG
H6	–283 -------- –257	18/27	13/27		CCAACGCGTCGTTCGCGAGAACGCGGC
H7	–227 -------- –207	10/11	10/11		GCATGCGCATT
H8	–210 -------- –203	8/8	7/8		AACAACAA
H9	–192 ---------181	8/12	7/12	SP1	CCAGCCCCGCCC
H10	–168 ---------157	10/12	7/12	AP2	CATTCAGGCTTC
H11	–158 -------- –147	10/10	10/10	NFY	CCATTGGCTG
H12	–113 -------- –107	7/7	7/7	NFY (CCAAT)	GACCAAT
H13	–93-------- –83	10/11	10/11	AP2	GGGCGTGCCCG
H14	–60 -------- –51	9/10	9/10		GCCTCGCGCG
H15	–48 -------- –36	13/13	13/13		CCATTGGTCGGCT
H16	–31 -------- –15	17/17	16/17	SP1	GAGGGGAGGAGCCGCTG
H17	–8 -------- +6	13/14	13/14	SP1	CCGCCGAGATGAGC
H18	+85 -------- +95	8/11	7/11		GTGGGCTACTG
H19	+120 -------- +146	21/27	14/27		GGCGGGGTTCGGAGTCGGGTCACCGTA
H20	+171 -------- +181	8/11	6/11		GGGATCGGTTA
H21	+182 -------- +194	10/13	9/13	STRE	GCTAGAGAAGGGG
H22	+232 -------- +241	7/10	6/10		CGGGGTTGAA
H23	+250 -------- +262	11/13	10/13		GGCCTCGGCGCGG
H24	+283 -------- +294	8/12	8/12		ACCGGTGTCGGG
H25	+306 -------- +329	20/24	18/24		GGGCTCTGACCTGGTCACGCGCCC
H26	+331 -------- +338	7/8	6/8	SP1	GCCCGGCC
H27	+340 -------- +354	15/15	13/15	CREB	GGTGCGTCACAGTCG
H28	+361 -------- +376	12/16	11/16	AP1	CCTTGGCTACCGGCTC
H29	+377 -------- +399	20/23	20/23		TTTGTCCCCGCGCTGTGCTTGGG

Underlines in sequences are identical bases between mouse, pig and human.

luciferase vector S7. These results indicated that the region from –1427 to –176 might contain the negative regulatory region of the promoter activity of non-mitochondrial PHGPx.

Functional Analysis of the Promoter Region of Mitochondrial PHGPx—To clarify the core and *cis*-regulatory regions in mitochondrial PHGPx, we made a series of 5′ and 3′ deletion mutants of the mitochondrial PHGPx promoter linked to the luciferase gene M1 in consideration of the homology domain. Figure 3A shows the sites of deletions in the construct of the luciferase vector. Figure 3B shows the relative luciferase activities in mouse L929 cells, compared with basic promoterless luciferase vector C. A construct M8 (–1427/–234) by 3′ deletion of a region (–233/–146), including the homology domain H7 to H11 from a construct M1 shows no luciferase activity compared to the basic promoterless luciferase vector C, although a construct M7 (–1427/–158) by 3′ deletion of a region (–159/–146) including H11, the NFY binding site, from a construct M1 shows twice higher luciferase activities compared to that of a construct M1 with the NFY binding site. Since the luciferase activity of a construct M6 by 5′ deletion of a region (–1427/–281) including H1 to H5 from a construct M1 was the same level as that of a construct M1, the region (–280/–146), including H6 to H11, is sufficient for the core promoter activity of mitochondrial PHGPx. These results suggest that the core promoter region of mitochondrial PHGPx is mediated mainly by the region (–233/–158) in the 5′ flanking region of mitochondrial PHGPx. The regions include four homology domains (H7 to H10), including two putative SP1 and AP2 binding sites. The construct M9 made by mutation from TTGGC at –153/–149 to ACTTG in the NFY binding site of the H11 domain of a construct M5 showed no change in the level of luciferase activity of a construct of luciferase vector M5 (Fig. 3 and Table 4). These results indicated that the NFY binding site in the H11 domain is not essential for the core promoter activity of mitochondrial PHGPx.

On the other hand, the luciferase activity of a construct M5 by 5′ deletion of a region (–1427/–359) including H1 and H2 from a construct M1 was significantly increased, whereas the increased activity was decreased by 5′ deletion of a region (–358/–281) including H3 to H5 from a construct M5. These results indicated that the region (–358/–281) included the positive regulatory region for mitochondrial PHGPx, but that up-regulation by this region was suppressed by the upstream negative regulatory region

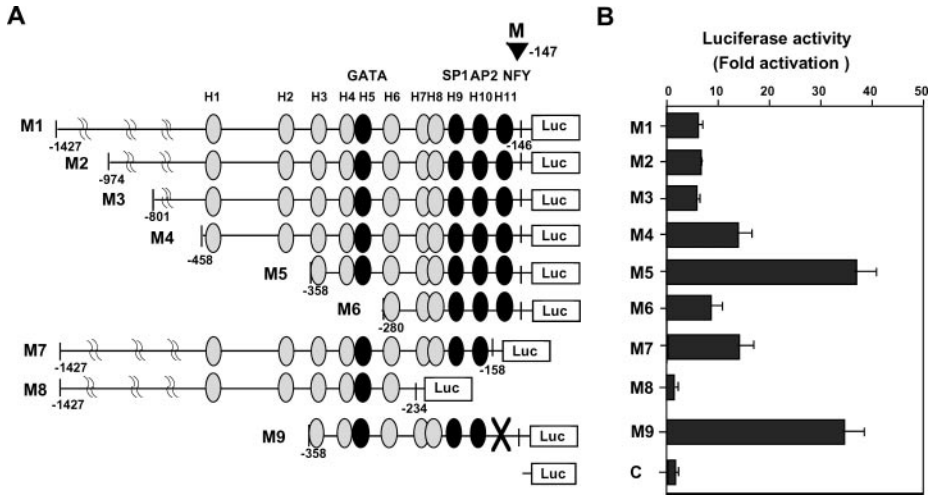

Fig. 3. **Deletion and mutational analysis of the promoter region of mitochondrial PHGPx.** (A) Construction of reporter gene vectors of mitochondrial PHGPx by deletion and mutation analysis. The number indicates that the gene base pair of PCR fragments of the 5′-flanking regions of mitochondrial PHGPx (M) used for reporter gene construction. M1-9 includes the promoter region of mitochondrial PHGPx. The black and gray circles are homology domains with and without putative transcriptional factor binding sites by analysis of the TRANSFAC program. X in M9 vector is the mutation site in the NFY binding region within the H11 homology domain, as shown in Table 4. (B) Relative luciferase activity of the different promoter constructs of mitochondrial PHGPx corrected for firefly luciferase activity in L929 cell lines. Cells were transfected with different constructs using a lipofectoamine plus transfection kit. To correct luciferase activity measured for transfection efficiency, cotransfections with a control plasmid containing renilla luciferase were carried out. The relative luciferase activity of the negative control (C; pGL3 basic vector) is indicated as 1.0.

(–801/–359) in somatic cells under normal culture conditions. We observed the same results for luciferase activity in mouse Y1 cells using constructs of M1–M8 as in mouse L929 cells (data not shown).

Functional Analysis of the Promoter Region of Non-Mitochondrial PHGPx—To clarify the core and *cis*-regulatory regions in non-mitochondrial PHGPx, we made a series of 5′ and 3′ deletion mutants of the non-mitochondrial PHGPx promoter linked to the luciferase vector S1 in consideration of the homology domain (Fig. 4A). As shown in Fig. 2C, luciferase activity from a construct S1 only reflected the promoter activity of non-mitochondrial PHGPx. Figure 4A shows the site of the deletions in the construct of the luciferase vector. Figure 4B shows the relative luciferase activities in mouse L929 cells, compared with basic promoterless luciferase vector C.

The luciferase activity of a construct S4 by 5′ deletion of a region (–1427/–370) including H1 and H2, from a construct S1 was significantly increased, whereas the increased activity was decreased to the basic activity of a construct S1 by 5′ deletion of a region from (–369/–281) including H3 to H5 from a construct S5. These results indicated that the region (–358/–281) included the positive regulatory region of non-mitochondrial PHGPx, but that the enhancer was suppressed by the upstream suppressor region (–458/–370) in somatic cells under normal culture conditions. This positive regulatory region in Fig. 4B was the same as that of mitochondrial PHGPx in Fig. 3B. On the other hand, the luciferase activity of a construct S7 by 5′ deletion of a region (–280/–177) including H6 to H9, from a construct S6 was significantly increased to the maximal luciferase activity of non-mitochondrial PHGPx. However, the luciferase activity of a construct S8 was decreased to the basic activity of a construct S1 by 5′ deletion of a region (–176/–126) including H10 and H11, the AP2 and NFY binding sites, from a construct S7. These results indicated that the region (–176/–126) including AP2 and NFY is required for the full luciferase activity of non-mitochondrial PHGPx. A construct S10 (–8/+39) by 5′ deletion of a region (–60/–9) including H14 to H16 from a construct S9 shows no luciferase activity compared to the basic promoterless luciferase vector C, although a construct S9 (–60/–39) by 5′ deletion of a region (–125/–61) including H12 and H13, NFY (CCAAT) and AP2 binding sites, from a construct S8 showed the basic same activity as that of a construct S1 of non-mitochondrial PHGPx. These results indicate that the region (–60/–9) including H14 to H16 is the core promoter for non-mitochondrial PHGPx. The region (–8/–39) including H17, the SP1 binding site, is not required for the promoter activity of non-mitochondrial PHGPx.

A construct S7 showed the maximum luciferase activity of non-mitochondrial PHGPx by 5′ deletion of the promoter region. Surprisingly, a construct S11 (–176/–56) by 3′ deletion of a region (–55/+39) from a construct S7, including H14 to H17, had the same highest luciferase activity as that of the construct S7. On the other hand, a construct S12 (–176/–114) by 3′ deletion of a region (–115/–56) including H12 and H13, the NFY (CCAAT) and AP2 binding sites, from a construct S11 showed a decrease of activity to the basal promoter level of a construct S1. These results indicate that the maximum promoter activity of non-mitochondrial PHGPx is required for the two regions (–176/–126 and –115/–56). We observed the same luciferase activity results in mouse Y1 cells using constructs of S1–S18, as those in mouse L929 cells (data not shown).

Next we examined the effects of mutation of the NFY binding site in H11 and H12 and the AP2 binding site in H13 on the maximum promoter activity of constructs S4

Table 4. **Sequences of probes and primers.**

Probes for gel shift assay	
k	5′-CCTTCATTCAGGCTTCCCATTGGCTGCAGG-3′
NFY-c	5′-GTGATTGGTTAA-3′
AP-2-c	5′-GCCCGCGG-3′
m	5′-TCTGACCAATAAGAGACGTCAGTGGGCGTGCCCG-3′
x	5′-GCGGGCTCTGACCTGGTCACGCGCCCTGCCCGGCCT-3′
SP1-c	5′-GGGGCGGGGC-3′
y	5′-GGTGCGTCACAGTCGGCGGCGCCTTGGCTACCGGCTC-3′
f	5′-TCCCAGAGGTTCCCCAAAGCGCCCTGGCACCCT-3′
fm1	5′-TCCGAGAGGTTCCCCAAAGCGCCCTGGCACCCT-3′
fm2	5′-TCCCAGAGGGTCCCCAAAGCGCCCTGGCACCCT-3′
fm3	5′-TCCCAGAGGTTCTTTAAAGCGCCCTGGCACCCT-3′
fm4	5′-TCCCAGAGGTTCCGCAAAGCGCCCTGGCACCCT-3′
fm5	5′-TCCCAGAGGTTCCCCAAATCGCCCTGGCACCCT-3′
STAT-c	5′-GAGCCTGATTTCCCCAAATGATGAGCTAG-3′
STAT-m	5′-GAGCCTGATTTCTTTGAATGATGAGCTAG-3′
Primers for mutation of promoter analysis	
NFY in H11 (M9, S13 and S16)	5′-TCATTCAGGCTTCCCAACTTGTGCAGGGGCCTCGCG-3′
NFY in H12 (S14 and S17)	5′-CGCAGGCGCATCTGATCGATAAGAGACGTCAGT-3′
AP2 in H13 (S15 and S16)	5′-GACGTCAGTGGGCGTTTTTGAGGGCGGGCAAGCC-3′
SP1 in H26 (N8)	5′-TGGTCACGCGCCCTGAAAGGCCTGGTGCGTCACA-3′
CREB in H27 (N9)	5′-CCTGCCCGGCCTGGTGGCTAGCAGTCGGCGGCGCCTTG-3′
M13	5′-AAAGGTACCTTCCGAGAGGTTCCCCAAAGCG-3′
M14	5′-AAAGGTACCTTCCCAGGGGTTCCCCAAAGCG-3′
M15	5′-AAAGGTACCTTCCCAGAGGGTCCCCAAAGCG-3′
M16	5′-AAAGGTACCTTCCCAGAGGTTCTTTAAAGCGCCCTGG-3′
M17	5′-AAAGGTACCTTCCCAGAGGTTCCGCAAAGCG-3′
M18	5′-AAAGGTACCTTCCCAGAGGTTCCCCAAATCGCCCTGG-3′

Underlines are mutation sites from original sequences.

and S7 of non-mitochondrial PHGPx (Fig. 4, C and D, and Table 4). The constructs S13 and S16 made by mutation from TTGGC at –153/–149 to ACTTG in the NFY binding site of the H11 domain of the constructs S4 and S7 resulted in a significant decrease to 20% of the level of the luciferase activities of the constructs S4 and S7. The constructs S15 and S18 made by mutation from GCCC at –87/–84 to TTTT in the AP2 binding site of the H13 domain of the constructs S4 and S7 resulted in a significant decrease to a half of the level of the luciferase activities of the constructs S4 and S7. On the other hand, the constructs S14 and S17 made by mutation from CCAAT at –111/–107 to TCGAT in the NFY binding site of the H12 domain of the constructs S4 and S7 showed no change in the level of luciferase activities of the constructs S4 and S7. These results indicate that the maximum promoter activity of non-mitochondrial PHGPx is required for the two sites, the NFY binding site in the H11 domain and the AP2 binding site in the H13 domain.

Functional Analysis of the Promoter Region of Nucleolar PHGPx—To clarify the core and *cis*-regulatory regions in nucleolar PHGPx, we made a series of 5′ and 3′ deletion mutants of the nucleolar PHGPx promoter linked to the luciferase gene N1 in consideration of the homology domain. Figure 5A shows the site of the deletions in the construct of the luciferase vector. Figure 5B shows the relative luciferase activities in mouse L929 cells, compared with basic promoterless luciferase vector C. A construct N6 (+84/+342) by 3′ deletion of a region (+343/+401) including H27 to H29, the cAMP response element binding site (CREB) and the AP-1 binding site, from a construct N1, show no luciferase activity compared to the basic promoterless luciferase vector C, although a construct N2 (+84/+375) by 3′ deletion of a region (+376/+401) including H29 from a construct N1 shows no decrease of luciferase activities of the basic promoter activity of nucleolar PHGPx. The construct N9 made by mutation from CGTCAC at+344/+349 to GCTAGC in the CREB binding site of the H27 domain of a construct N4 resulted in a significant decrease to 35% of the level of the luciferase activity of a construct N4 (Fig. 5 and Table 4). These results indicated that the region (+342/+375) including the CREB is essential for the core promoter activity of nucleolar PHGPx in L929 cells. The luciferase activity of a construct N4 by 5′ deletion of a region (+84/+243) including H18 to H22 from a construct N1 was two times higher than that of a construct N1, whereas the activity of a construct N5 was decreased by 5′ deletion of a region (+244/+271) including H23 from a construct N4. These results indicate that the region (+244/+271) is the positive regulatory region of nucleolar PHGPx, but that the up-regulation by this region is suppressed by the upstream negative regulatory region (+84/+175) in somatic cells under normal culture conditions. The construct N8 made by mutation from CCC at –87/–84 to AAA in the SP1 binding site of the H26 domain of a construct N4 resulted in a significant decrease to the 25% of the level of the luciferase activity of a construct N4 (Fig. 5 and Table 4). These results indicated that the SP-1

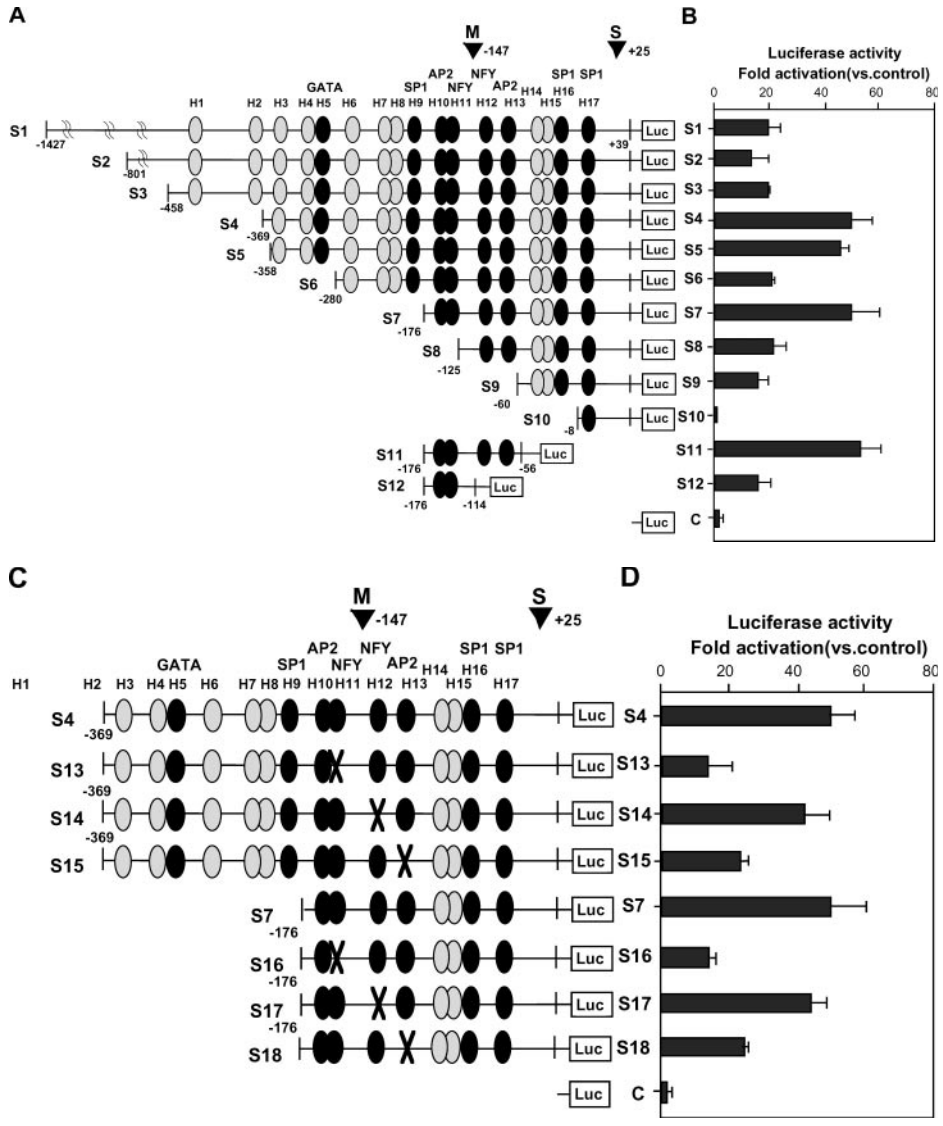

Fig. 4. **Deletion and mutational analysis of the promoter region of non-mitochondrial PHGPx.** (A and C) Construction of reporter gene vectors of non-mitochondrial PHGPx by deletion (A) and mutation (C) analysis. The number indicates the gene base pair of PCR fragments of the 5′-flanking regions of non-mitochondrial PHGPx (S) used for reporter gene construction. S1–6 and S13–15 include the promoter regions of both mitochondrial and non-mitochondrial PHGPx. S7–12 and S16–18 included the only promoter region of non-mitochondrial PHGPx. The black and gray circles are homology domains with and without putative transcriptional factor binding sites by analysis of the TRANSFAC program. (C) Xs are mutation sites in NFY and AP2 binding region within the H11–H13 homology domain, as shown in Table 4. (B and D) Relative luciferase activity of the different promoter constructs of non-mitochondrial PHGPx corrected for firefly luciferase activity in L929 cell lines. Cells were transfected with different constructs using a lipofectoamine plus transfection kit. To correct luciferase activity measured for transfection efficiency, cotransfections with a control plasmid containing renilla luciferase were carried out. The relative luciferase activity of the negative control (C; pGL3 basic vector) is indicated as 1.0.

binding site in the H26 domain is essential for the maximum promoter activity of nucleolar PHGPx in L929 cells. We observed the same luciferase activity results in mouse Y1 cells using constructs of N1–N7 as those in mouse L929 cells (data not shown).

Identification of the Binding of Putative Transcriptional Factors to the Core Regions of the Three Promoters of PHGPx in L929 Cells—To investigate whether putative transcriptional factors bind to each core and *cis*-regulatory region of each type of PHGPx in L929 cells, we performed electrophoretical mobility shift analysis (EMSA) using the nuclear extracts of L929 cells and supershift assay using specific antibodies as shown in Fig. 6 and Table 4. Probe k contains an AP2 binding site in the H10 domain of the core promoter region of mitochondrial PHGPx, as shown in Fig. 3, and Probe k also contains the NFY binding site of the H11 domain in the *cis*-regulatory region of maximum promoter activity of non-mitochondrial PHGPx, as shown in Fig. 4 and Table 4. EMSA using probe k indicated a two shift band when the nuclear extracts from L929 cells were used as the source of the binding protein. Addition of an AP2 antibody caused the disappearance of both the bands of probe k. Addition of a NFY antibody caused a super shift of both the bands of probe k. These results indicated that AP2 bound to the core promoter region of mitochondrial PHGPx and NFY bound to the *cis*-regulatory region for maximum promoter activity of non-mitochondrial PHGPx. Probe m contains NFY (CCAAT) and AP2 binding sites in the H12 and H13 domains of the *cis*-regulatory region of non-mitochondrial PHGPx, as shown in Fig. 4 and Table 4. EMSA using probe m indicated two shift bands when the nuclear extracts from L929 cells were used as the source of the binding protein. Addition of an AP2 antibody caused faintness or the disappearance of both the bands of probe m. Addition of a NFY antibody caused a super shift of the bands of probe m. However, the addition of a C/EBP antibody caused no change in the bands of probe m, although the sequence of probe m contained a putative C/EBP binding site in the mouse gene, but not in pig and human genes. These results indicated that AP2 and NFY bound to the *cis*-regulatory region of non-mitochondrial PHGPx, but not C/EBP. Probe x

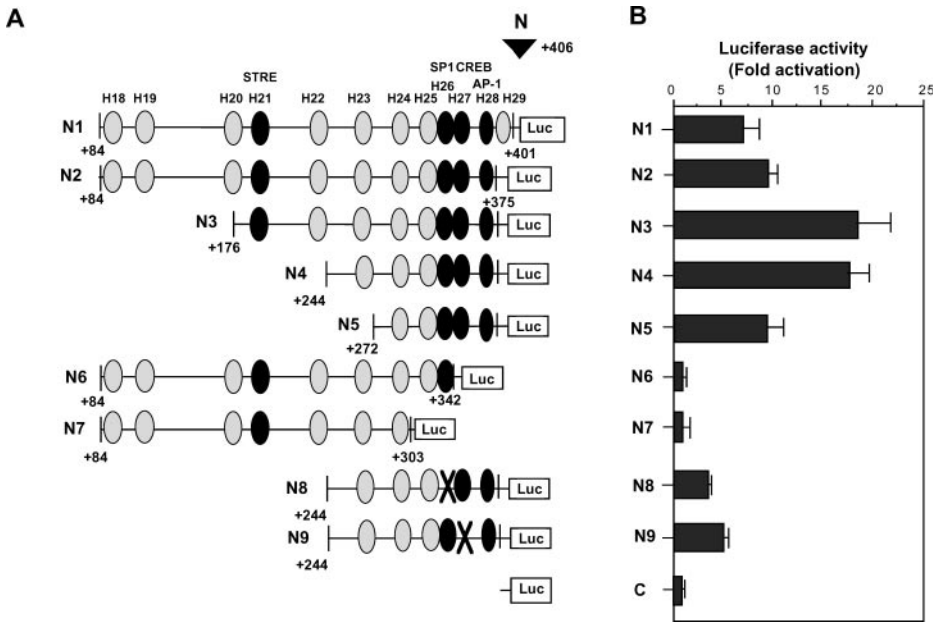

Fig. 5. **Deletion and mutational analysis of promoter region of nucleolar PHGPx.** (A) Construction of reporter gene vectors of nucleolar PHGPx by deletion analysis. The number indicates the gene base pair of PCR fragments of the 5′-flanking regions of nucleolar PHGPx (N) used for reporter gene construction. N1-9 includes the promoter region of nucleolar PHGPx. The black and gray circles are homology domains with and without putative transcriptional factor binding sites by analysis of the TRANSFAC program. Xs are mutation sites in SP1 and CREB binding region within the H26 and H27 homology domain as shown in Table 4. (B) Relative luciferase activity of the different promoter constructs of nucleolar PHGPx corrected for firefly luciferase activity in L929 cell lines. Cells were transfected with different constructs using a lipofectoamine plus transfection kit. To correct luciferase activity measured for transfection efficiency, cotransfections with a control plasmid containing renilla luciferase were carried out. The relative luciferase activity of the negative control (C; pGL3 basic vector) is indicated as 1.0.

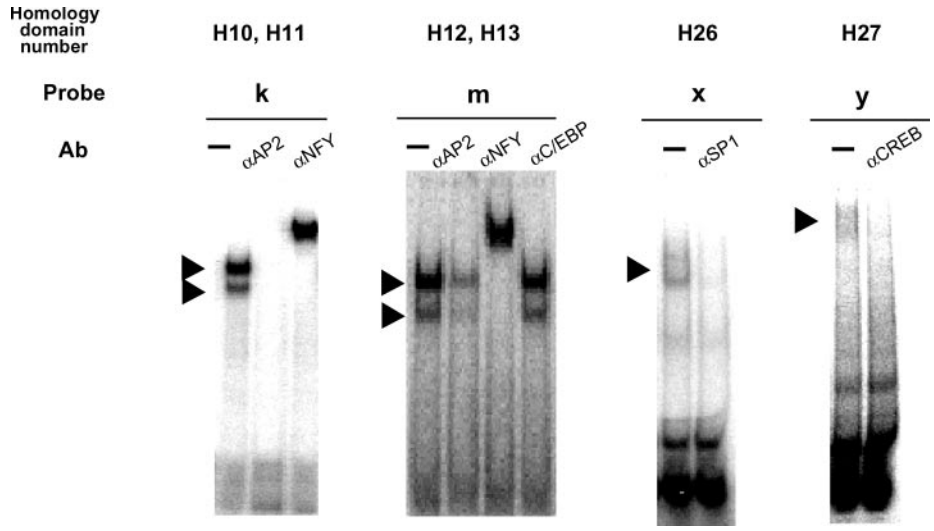

Fig. 6. **Electrophoretical mobility shift analysis of the core region of three types of PHGPx.** The labeled oligonucleotide probes (k, m, x and y) containing each homology domain (H10–H13, H26 and H27) of the 5′-flanking region of the PHGPx gene (see Tables 3 and 4) were incubated with nuclear extracts of L929 cells. After 30 min incubation at 4°C, the entire binding sample was applied to polyacrylamide gel electrophoresis. Arrowheads indicated DNA-protein complexes. For the supershift experiments shown in this figure, specific antibodies raised against SP1, NFY, AP2, C/EBP and CREB were added to the incubation mixtures.

contains a SP1 binding motif in the H26 domain of the *cis*-regulatory region for maximum promoter activity of nucleolar PHGPx, as shown in Fig. 5 and Table 4. EMSA using probe x indicated a single shift band. Addition of a SP1 antibody caused the disappearance of the shift bands of probe x. Probe y contains a CREB binding motif in the H27 domain of the core promoter region of nucleolar PHGPx, as shown in Fig. 5 and Table 4. EMSA using probe y indicated a single shift band as shown in Fig. 6. Addition of a CREB antibody caused a disappearance of the shift bands of probe y. These results indicated that SP1 and CREB binding proteins bound to the *cis*-regulatory and core promoter region of nucleolar PHGPx.

Identification of Transcriptional Factor Binding Sites in the Positive Regulatory Region of Mitochondrial PHGPx—As shown in Fig. 3, we determined the existence of positive regulatory regions (–358/–281) in the 5′-flanking region of mitochondrial PHGPx. To identify transcriptional factor binding sites in the positive regulatory regions of

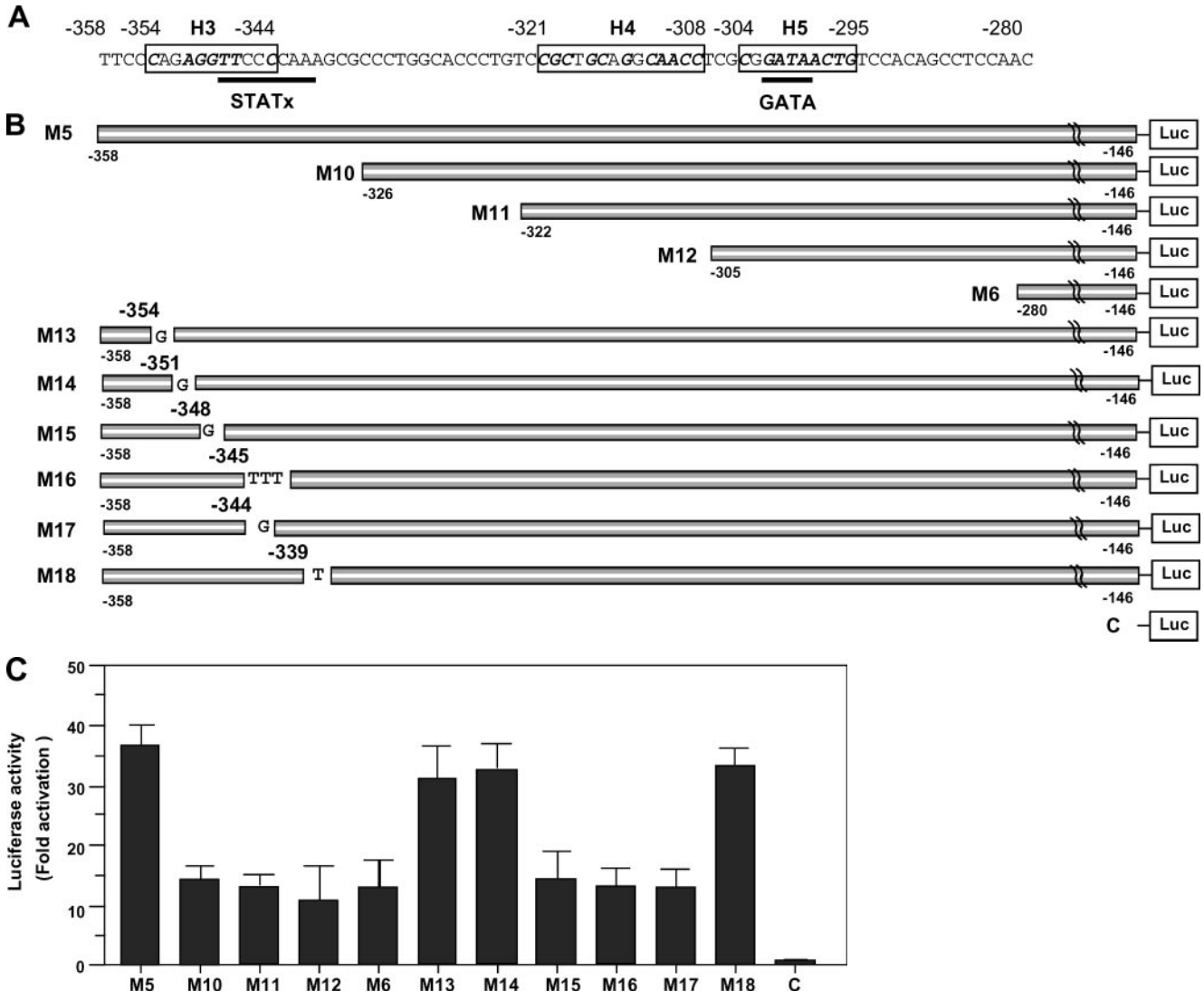

Fig. 7. **Deletion and mutational analysis of the positive regulatory region of mitochondrial PHGPx.** (A) Putative transcriptional factor binding sites and homology domains of the positive regulatory region (–358/–280) of the PHGPx gene. The three boxes are three homology domains (H3, H4 and H5) among human, pig and mouse in the positive regulatory region of mitochondrial PHGPx. Underlines show the putative transcriptional factor binding sites, STAT and GATA. Italic bold letters are identical bases between mouse, pig and human. (B) Construction of reporter gene vectors in positive regulatory regions of mitochondrial PHGPx for 5′ deletion and mutational analysis. The number indicates the gene base pair of PCR fragments of the 5′-flanking regions used for reporter gene construction. M10–M12 includes the deletion constructs from the M5 luciferase vector. M13–M18 indicates that the mutational constructs in H3 homology domains are derived from the M5 luciferase vector. (C) Relative luciferase activity of the different promoter constructs of the positive regulatory region of mitochondrial PHGPx corrected for firefly luciferase activity in L929 cell lines. Cells were transfected with different constructs using a lipofectoamine plus transfection kit. To correct luciferase activity measured for transfection efficiency, cotransfections with a control plasmid containing renilla luciferase were carried out. The relative luciferase activity of the negative control (C; pGL3 basic vector) is indicated as 1.0.

mitochondrial PHGPx, we made several constructs containing 5′ deletion and point mutations of the positive regulatory regions (–358/–281) of mitochondrial PHGPx from the luciferase construct M5 in consideration of the homology domain. Figure 7A shows the three homology domains (H3, H4 and H5) and two putative transcriptional factor binding sites, STAT and GATA, in the enhancer region of mitochondrial PHGPx. However, the putative STAT binding site exists only in the mouse gene, not in pig or human. Figure 7B shows the sites of deletions and point mutations in constructs of the luciferase vectors M10–M18. Figure 7C shows the relative luciferase activities in mouse L929 cells, compared with basic promoterless luciferase vector C. The highest luciferase activity of a construct M5 decreased to the level of the luciferase activity of a construct of M6 by just the deletion of the (–358/–327) region. This region includes the H3 homology domain and the putative STAT binding site (Fig. 7A). The construct M15 and M17 made by point mutation from T at –348 to G and from C at –344 to G and the construct M16 made by

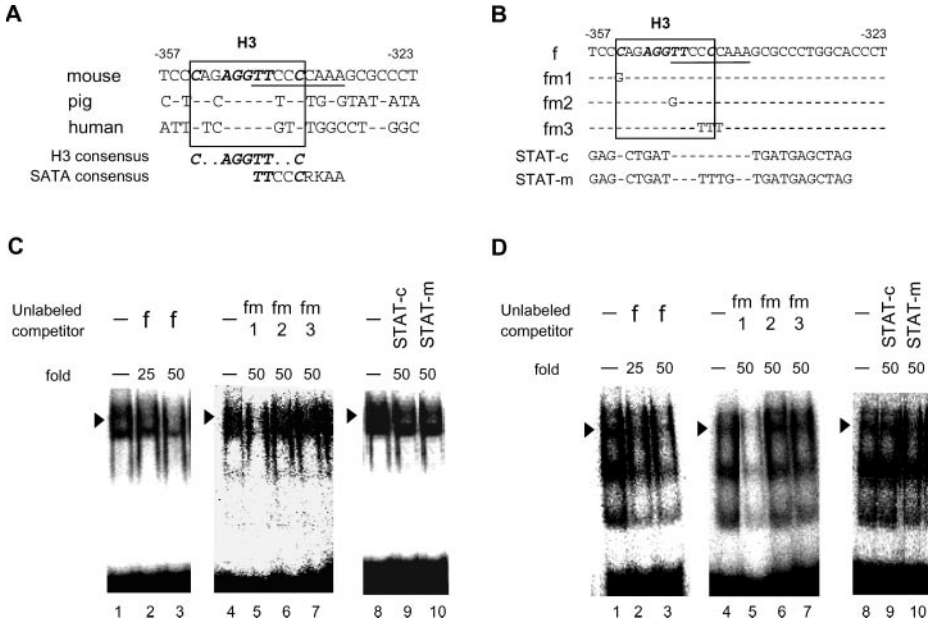

Fig. 8. **Electrophoretical mobility shift analysis of the positive regulatory region of mitochondrial PHGPx.** (A) Alignment of sequences of the mouse H3 homology domain among several species. Italic bold letters are identical bases between mouse, pig and human. An underline indicates a putative STAT binding site. (B) Oligonucleotide sequences of wild type (f) and mutant probes (fm1–3). Small bars are identical bases of f probe. Box indicate an H3 homology domain. Underlines indicate consensus sequences of a STAT binding site. STAT-c is a STAT consensus probe and STAT-m is a STAT mutational probe. (C and D) Competition analysis of the positive regulatory region of mitochondrial PHGPx using an excess of unlabeled oligonucleotides. A ^{32}P-labeled f probe was incubated with nuclear extracts from mouse L929 (C) and mouse TT2 embryonic stem (D) cells. Arrowheads indicate that a DNA-protein complex (lanes 1, 4 and 8) without competitor in C and D. The ^{32}P-labeled f probe was incubated with nuclear extracts in the presence of 25 and 50-fold excesses of unlabeled f oligonucleotide (lanes 2 and 3, respectively) as competitors and in the presence of 50-fold excess of unlabeled mutated probes fm1 (lane 5), fm2 (lane 6) and fm3 (lane7), and STAT consensus (lane 9) and STAT mutated (lane 10) probes as competitors.

mutation from CCC at –345/–343 to TTT in the positive regulatory region of a construct M5 resulted in a significant decrease to the level of the luciferase activity of a construct of M6, although the construct M13, M14 and M18 made by a point mutation from C at –354 to G, from A at –351 to G and from G at –339 to T showed no change in the level of luciferase activity of a construct of luciferase vector M5 (Fig. 7C).

Figure 8A shows the alignment of the positive regulatory region (–357/–323) including the H3 homology domain in mouse, pig and human. Italic bold letters indicate identical bases. This consensus sequence was not identical to known transcription factor binding sites. The results in Fig. 7C indicated that C at –354 in the H3 consensus was not essential for up-regulatory activity. Putative STATx binding sites indicated by the underline were identified beside the H3 homology domain in mouse, but not in pig or human (Fig. 8A). To further investigate whether the novel transcription factor might bind to the H3 homology domain or if STAT might bind to the STAT binding site of the positive regulatory region, we carried out EMSA experiments using the nuclear extracts of L929 cells and mouse TT2 embryonic stem (ES) cells cultured with Leukemia inhibitory factor (LIF). In ES cells, STAT3 is activated by addition of LIF, translocated into nuclei and bound to the putative STAT binding sites in promoter regions of several proteins, for example junB (*26*). We used the nuclear extracts of ES cells activated with LIF as a positive control of activated STAT. We prepared original oligonucleotides, f, covering the region between –357 and –323, three substitution oligonucleotides, fm1, C–354G, fm2, T–348G and fm3, –345CCC–343/TTT, a STAT consensus (STAT-c) and mutant STAT oligonucleotide (STAT-m) (Fig. 8B). The f probe could bind nuclear protein extracted from mouse L929 cells (Fig. 8C) and mouse TT2 ES cell (Fig. 8D). The band was competitively inhibited by a corresponding excess of unlabeled oligonucleotides, f, in a dose-dependent manner, as shown in Fig. 8, C and D. Furthermore, this band disappeared competitively in a 50-fold excess of unlabeled fm1 probe, but not in the presence of an excess of unlabelled fm2 and fm3 probes (Fig. 8, C and D). An excess of the consensus oligonucleotides of STAT and of the mutant oligonucleotides of STAT could not abolish the binding activity of the f probe in L929 and TT2 ES cells (Fig. 8, C and D).

To confirm that there was no binding of STAT to the f probe, we performed a super-shift assay using specific antibodies against STATx. The DNA-protein complex using the f probe in L929 and TT2 ES cells was not supershifted by anti-STAT1, anti-STAT3 and anti–STAT-4 antibodies (data not shown). On the other hand, The STAT3 probe-protein complex using the STAT3 consensus probe was supershifted by anti-STAT-3 antibodies in L929 and TT2 ES cells cultured with LIF (data not shown). These results indicated that novel nuclear factor complexes other than STAT might bind to the H3 homology domain in f, but not the putative STAT binding domain in L929 and TT2 ES cells.

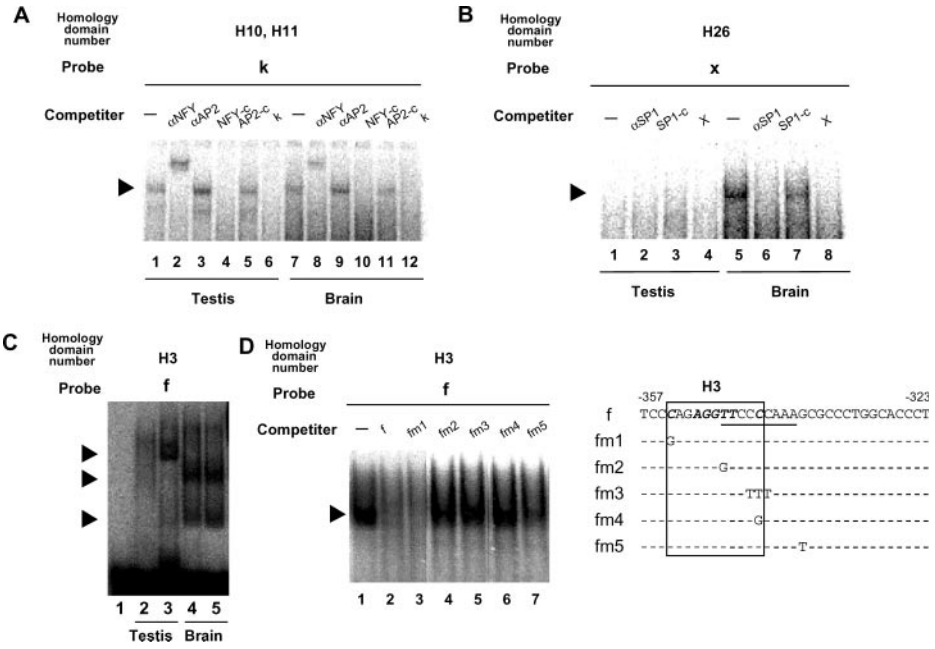

Fig. 9. **Electrophoretical mobility shift analysis in nuclear extracts of testis and brain in BALB/c mice using oligonucleotides containing positive regulatory region and core region of 5′-flanking regions of three types of the PHGPx gene as labeled probes.** (A) Characterization of transcription factor complexes bound to probe k containing the H10 and H11 homology domain in testes (lanes 1–6) and brain (lanes 7–12) of adult BALB/c mice (6 weeks old) by interference assay. The arrow indicates the probe k-protein complex in the absence of a competitor (lanes 1 and 7). The ^{32}P-labeled probe k was then incubated with nuclear extracts in the presence of a 50-fold excess of unlabeled probe k (lanes 6 and 12), consensus NFY probe (lanes 4 and 10), consensus AP-2 probe (lanes 5 and 11), anti-NFY (lanes 2 and 8) or anti–AP-2 (lanes 3 and 9) as a competitor. (B) Characterization of transcription factor complexes bound to probe x containing the H26 homology domain in testes (lanes 1–4) and brain (lanes 5–8) of adult BALB/c mice (6 weeks old) by interference assay. The arrow indicates the probe x-protein complex in the absence of a competitor (lanes 1 and 5). The ^{32}P-labeled probe x was then incubated with nuclear extracts in the presence of a 50-fold excess of unlabeled probe x (lanes 4 and 8), consensus SP-1 probe (lanes 3 and 7) or anti–SP-1 (lanes 2 and 6) as a competitor. (C and D) Characterization of transcription factor complexes bound to probe f containing the H3 homology domain in testes and brain by interference assay. (C) The ^{32}P-labeled probe f was then incubated without (lane 1) or with nuclear extracts from the testes (lanes 2 and 3) and brain (lanes 4 and 5) of young (2 weeks old; lanes 2 and 4) and adult (6 weeks old; lanes 3 and 5) BALB/c mice. The arrows indicate a specific transcription factor complex that binds to probe f in adult testis (lane 3) and two bands in young and adult brain (lanes 4 and 5). (D) Competition analysis using an excess of unlabeled oligonucleotides of the wild-type f and mutant fm1-fm5 probes. A ^{32}P-labeled wild-type f probe was incubated with nuclear extracts from the testes of adult BALB/c mice (6 weeks old). The arrow indicates the DNA protein complex in the absence of a competitor (lane 1). The ^{32}P labeled wild-type f probe was then incubated with nuclear extracts in the presence of a 50-fold excess of unlabeled wild-type probe f (lane 2) or mutant probes fm1–fm5 (lanes 3–7) as a competitor. In right panel, oligonucleotide sequences of wild type (f) and mutant probes (fm1–5). Small bars are identical bases of f probe. Italic bold letters are identical bases between mouse, pig and human. Box indicate H3 homology domain. Underline indicates consensus sequences of a STAT binding site.

Characterization of Transcription Factor Complexes Bound to Positive Regulatory and Core Regions of the Promoters of the Three Types of PHGPx between Testis and Brain by Electrophoretical Mobility Shift Analysis—To investigate whether different kinds or different amounts of transcriptional factors bind or not to each core and positive regulatory region of PHGPx between testis and somatic tissue such as brain, we performed electrophoretical mobility shift analysis (EMSA) using nuclear extracts of adult testis and brain in the positive regulatory region and core promoter regions we identified in this study. We used five gel shift probes (f, k, m, x and y as shown in Table 4) that covered the H3 positive regulatory domain, the H10 and H11 regulatory domain of mitochondrial PHGPx and non-mitochondrial PHGPx, the H12 core promoter domain of non-mitochondrial PHGPx, the H26 regulatory domain of nucleolar PHGPx and the H27 core promoter domain of nucleolar PHGPx. EMSA using probe k indicated a single band in the nuclear extracts from both adult testis and brain (Fig. 9A). Addition of an NFY antibody caused a super shift in the bands of both testis and brain, but addition of an AP2 antibody caused no change in the bands of both testis and brain. The bands of both testis and brain were competitively inhibited by a corresponding excess of unlabeled probe k and consensus oligonucleotides of NFY, but not unlabeled consensus oligonucleotides of AP2. These results indicated that NFY bound to *cis*-regulatory region for maximum promoter activity of non-mitochondrial PHGPx in adult testis and brain of mice, but AP2 did not bind to core region of mitochondrial PHGPx in both testis and brain. Probe m contains a NFY binding site in the H12 domain and a AP2 binding site in the H13 domain. EMSA using probe m indicated a single faint band in the nuclear extracts from both adult testis and brain, but we could not confirm the involvement of NFY and AP2 in the faint band by interference assay (data not shown).

Probe x contains an SP-1 binding site in the H26 domain. EMSA using probe x indicated a single band in the nuclear

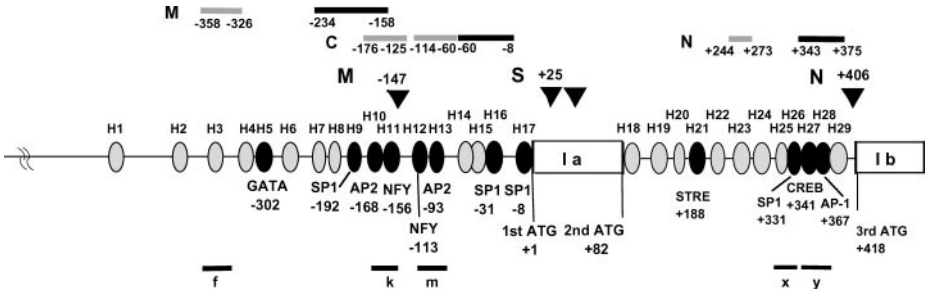

Fig. 10. **Summary of the identified regulatory and core promoter regions of 5′-flanking regions of exon Ia and exon Ib of the PHGPx gene in L929 cells.** Shadow bars on the upper side indicate the each regulatory region of the three types of PHGPx. Black bars in the upper side indicate the each core region of the three types of PHGPx. The number of the homology domains (H) is shown in Table 3. The black and gray circles are homology domains with and without putative transcriptional factor binding sites, respectively, by analysis with the TRANSFAC program. The black bars with letters on the lower side show the region for the probes used for electrophoretical mobility shift analysis in this study. Probes are summarized in Table 4.

extracts from adult brain, but not from adult testis (Fig. 9B). Addition of an SP1 antibody caused a disappearance in the bands of adult brain. The bands in adult brain were competitively inhibited by a corresponding excess of unlabeled probe x and consensus oligonucleotides of SP-1. These results indicated that SP1 bound to *cis*-regulatory region for maximum promoter activity of nucleolar PHGPx in adult brain, but not in adult testis. Probe y contains CREB binding site in the H27 domain. EMSA using probe y indicated a single faint band in the nuclear extracts from both adult testis and brain, but we could not confirm the involvement of CREB in the faint band by interference assay (data not shown).

Probe f contains the H3 homology domain of the positive regulatory region of mitochondrial and non-mitochondrial PHGPx in L929 and Y1 cells. The level of mitochondrial PHGPx mRNA is remarkably low in testis of young mice (2 weeks old) and adult somatic tissues as shown in Table 2. However, the level of mitochondrial PHGPx mRNA is significantly induced in testis during spermatogenesis from 3 week old mice and is saturated at 6 weeks old. Interestingly, EMSA using probe f indicated a single band in the nuclear extracts from adult (6 weeks old) testis, but not from young (2 weeks old) testis (Fig. 9C). On the other hand, EMSA using probe f indicated that two shift bands were detected in both nuclear extracts from adult and young brain and the size of the band-shifts were significantly different between testis and brain (Fig. 9C). These results suggested that different transcriptional factor complexes might bind to the probe f containing H3 positive regulatory domain and regulate the promoter activities of mitochondrial PHGPx and non-mitochondrial PHGPx between testis and brain.

To investigate the recognition sequence of a novel transcriptional factor bound to probe f in adult testis, we carried out EMSA interference assay using the nuclear extracts of adult testis (Fig. 9D). The probe f–testis protein complex was competitively inhibited by a corresponding excess of unlabeled oligonucleotides, f. Furthermore, this band disappeared competitively in a 50-fold excess of unlabeled fm1 and fm5 probe, but not in the presence of an excess of unlabeled fm2, fm3 or fm4 (Fig. 9D). These results indicated that a novel transcription factor bound to probe f in testis could recognize the T at –348 and C at –344 in the H3 domain, but not C at –354 and G at –339 (Fig. 9D).

DISCUSSION

Identification of Homology Domains in 5′-Flanking Regions of the Three Types of PHGPx in Several Species—Expression of mRNA for non-mitochondrial PHGPx mRNA is high in somatic cells whereas expressions of mitochondrial and nucleolar PHGPx are extremely low in somatic tissue and cultured cells in Table 2. On the other hand, expressions of mitochondrial and nucleolar PHGPx mRNA are remarkably high in testis in Table 2. An earlier study of ours indicated that a defect in the expression of mitochondrial PHGPx is linked to human infertility (*11*). Unfortunately, the regulatory mechanisms of the high expressions of mitochondrial and nucleolar PHGPx mRNA in testis and that of the high expression of non-mitochondrial PHGPx in somatic cells such as brain are essentially unknown.

In this study, we determined and summarized the basal core and positive regulatory regions of three types of PHGPx in somatic culture cell lines by deletion and mutational promoter analyses (Fig. 10 and Table 3). We first identified 29 consensus sequences in the 5′-flanking region of PHGPx by comparing sequences of 5′ flanking regions of PHGPx among mouse, pig and human. Twelve regions of the 29 homology domains included the putative consensus binding sequences for several transcriptional factors, but 17 regions of these homology domains did not contain putative transcriptional factor binding sites.

Identification of the Positive Regulatory Region of Mitochondrial PHGPx—We identified, for the first time, the positive regulatory region in the H3 homology region of the 5′-flanking region of mitochondrial PHGPx by deletion and mutational promoter analysis (Figs. 3 and 7). Since the H3 homology region is overlapped with putative STAT consensus binding sites in mouse, but not in pig and human, we clarified that the transcription factor complexes binding to the H3 homology region contained novel transcriptional factor complexes, but not STAT in L929 and ES cells (Fig. 8). EMSA interference assay indicated that this novel transcriptional factor at least could recognize T at –348 and C at –344, but not C at

–354 in the H3 consensus domain (–354/–344: C.. AGGTT..C) (Fig. 7 and Fig. 8). The positive regulatory region could also increase the promoter activity of non-mitochondrial PHGPx (Fig. 4). The up-regulation of luciferase activities by this region in mitochondrial PHGPx and non-mitochondrial PHGPx are at the same levels as the highest activity of the core promoter in non-mitochondrial PHGPx (Figs. 3 and 4). The positive regulatory region is powerful for the enhancement of transcription of two types of PHGPx; however, its activity is suppressed by addition of the upstream region of mitochondrial PHGPx and non-mitochondrial PHGPx in somatic cells (Figs. 3 and 4). The enhancement activity against the promoter activity of mitochondrial PHGPx was lost when the H3 domain was placed on a 3′ side of the reporter gene (data not shown). These results indicated that this positive regulatory region was not typical for the enhancer. Mutation of the NFY site in the H11 domain in the promoter activity of mitochondrial PHGPx showed no change in the level of maximum promoter activity of mitochondrial PHGPx (Fig. 3). However, mutation of the NFY site in the H11 domain in the promoter activity of non-mitochondrial PHGPx resulted in a significant decrease of the level of the maximum promoter activity of non-mitochondrial PHGPx (Fig. 4). These results suggested that the expression of mitochondrial and non-mitochondrial PHGPx mRNA might be regulated by the positive and negative regulatory regions of a different mechanism.

To clarify whether probe f involving the H3 domain contains the regulatory region for the high level expression of mitochondrial PHGPx mRNA in testis, we carried out EMSA. The level of expression of mitochondrial PHGPx mRNA is very low in testis of young mice (2 weeks old). However, the level of expression of mitochondrial PHGPx mRNA is significantly induced during spermatogenesis in testis of adult mice (6 weeks old). A single band shift of probe f-protein complex was detected in adult (6 weeks old) mice, but not in young (2 weeks old) mice (Fig. 9C). The specificity of the binding of transcriptional factor complexes to the positive regulatory region in testis is the same as that in L929 cells (Figs. 8 and 9D). However, the size of the band-shifts in nuclear extracts of adult brain was significantly different from that in testis, but the same as that in young brain. These results suggested that different transcriptional factor complexes might bind to the probe f containing the H3 positive regulatory domain and regulate the promoter activities of mitochondrial PHGPx and non-mitochondrial PHGPx between testis and brain.

Characterization of the Core Promoter Regions of the Three Types of PHGPx in Somatic Cells—We identified the core regions of the promoters of the three types of PHGPx by deletion of homology domains from the 3′ end in the promoter region. The deletion of the H7–H11 domain of the promoter of mitochondrial PHGPx resulted in the loss of promoter activity, whereas the deletion and mutation of the NFY binding site in the H11 domain showed no decrease in the promoter activity of mitochondrial PHGPx (Fig. 3). We identified the binding of AP2 and NFY to H10 and H11, respectively, using nuclear extracts of L929 cells by gel shift and supershift analyses (Fig. 6). The H7 and H8 domain contains an unidentified transcriptional factor binding site. A recent report by Ufer *et al.* reported that mutational promoter analysis using only the 5′-flanking region from –247 to –12 indicated that the mutation of the SP1 site resulted in the severe loss of promoter activity, whereas mutation of NFY resulted in only a 20% decrease of promoter activity (*15*). Their results indicated that SP1 and NFY are essential for the core promoter activity of mitochondrial PHGPx; however, we demonstrated that the SP1 and AP2 binding sites are necessary for core promoter activity, but that the NFY binding site is not essential for the promoter activity of mitochondrial PHGPx (Fig. 5). We think that it is doubtful that the promoter activity of mitochondrial PHGPx proposed by Ufer et al. is correctly postulated, since their construct include the core promoter region from –147 to –12 of non-mitochondrial PHGPx, and the level of activity of the promoter of mitochondrial PHGPx was the same as that of the activity of non-mitochondrial PHGPx (*15*).

Our 5′ deletion promoter analysis of non-mitochondrial PHGPx indicated that the basal activity of non-mitochondrial PHGPx is essential for the region from –60 to –8, the H14–H16 domain (Fig. 4). Since we could not detect the binding of SP1 to the H16 domain by supershift analysis (data not shown), the H14 and H15 domains, with novel transcriptional factor binding sites, are necessary for basal core promoter activity. On the other hand, 3′ deletion promoter analysis indicated that the region from –176 to –114, containing the H10 and H11 domains, AP2 and NFY binding sites, had the basal promoter activity of non-mitochondrial PHGPx, but not the full activity. The highest promoter activity in non-mitochondrial PHGPx is necessary for the region from –176 to –60, all H10–H13 domains. These domains contain two AP2 and NFY binding sites including the CCAAT site (Figs. 4 and 9A). Our mutational promoter analysis indicated that NFY in the H11 domain and AP2 in the H13 domain are essential for the maximum promoter activity of non-mitochondrial PHGPx, but not NFY in the H12 domain (Fig. 4, C and D). On the other hand, mutational promoter analysis by Ufer *et al.* indicated that the promoter activity of non-mitochondrial PHGPx (from –247 to +53) is dropped by mutation of the SP1 site in the H9 domain, and by mutation of the NFY site in the H12 domain, but there is no effect of the mutation of the NFY site in the H11 domain. This discrepancy might be due to the difference of the constructs of the luciferase vectors (Fig. 2), since our constructs of luciferase vectors did not include the promoter activity of mitochondrial PHGPx; whereas Ufer *et al.*'s constructs overlapped the promoter activity of mitochondrial PHGPx with the promoter activity of non-mitochondrial PHGPx (*15*).

Deletion and mutational promoter analysis of nucleolar PHGPx has not been yet undertaken in mammalian cells. We have shown, for the first time, that the region from +342 to +375 including the CREB and AP-1 binding sites in the H27 and H28 domain is necessary for core promoter activity by 3′ deletion analysis (Fig. 5). We also found that the H23 domain was the positive-regulatory region for nucleolar PHGPx. However, this up-regulation region is normally suppressed by the upstream region in L929 cells, as the H23 domain contains an unidentified transcriptional factor binding site. Furthermore, the transcriptional factor complexes bound to the H23 domain remains to be identified.

Mutational analysis of SP1 in the H26 domain and CREB in the H27 domain resulted in a significant decrease of the promoter activity of nucleolar PHGPx in L929 cells. In L929 cells, we identified the transcriptional factor complexes bound to the H27 domain as CREB by supershift assay; however, we could not identify the transcriptional factor bound to the H27 domain in testis and brain by supershift assay. The family of nuclear transcription factors that contain a basic domain/leucine zipper motif (bZIP) that bound to a cAMP-response element (CRE), have two predominant members, the cAMP-response element binding protein (CREB) and the cAMP-response element modulator (CREM) (27,28). Several alternatively spliced forms (CREM-τ, $\tau_?$, τ_2) act as transcription activators, while other isoforms (CREM-α, β, γ) function as transcription suppressors (*27*). A high level of the activator isoforms CREM-τ is observed from the round spermatid onwards (*27*, *29*). A recent study has indicated that overexpression of CREM-τ, enhanced the promoter activity of nucleolar PHGPx in culture cells (*30*) and that the nuclear extract from rat spermatid cells can specifically bind to the CREB site in the promoter region of rat nucleolar PHGPx (*30*). We have not identified whether this transcription factor binding to the y probe in testis is CREM-τ or not; however, these results suggested that the CREB site is an important region for enhancement of the induction of transcription of nucleolar PHGPx.

In this study we demonstrated for the first time the existence of a positive regulatory region of mitochondrial PHGPx. This region has novel transcriptional factor binding sites and consensus sequences between pig, mouse and human. The region can regulate the promoter activities of non-mitochondrial PHGPx. However, in somatic cells, the region is suppressed by the upstream region under normal conditions. Mitochondrial PHGPx are highly expressed in testis, but have a significantly low expression in somatic tissues. The size of the transcription factor complexes bound to the positive regulatory region in testis is different from that in brain. These changes of the transcriptional factor complexes bound to the positive regulatory region might be linked to the higher expression of mitochondrial PHGPx in testis than that in brain. It remains to be clarified whether the positive regulatory region is really necessary for the induction of mitochondrial PHGPx during spermatogenesis, and whether the genetic mutation of the positive regulatory region is linked to human infertility.

We thank Miwako Hiwasa, Tomoko Yamada, Megumi Ajima, Yumi Kawamura and Mr. Yuujiro Yamato for expert technical assistance. This work was supported in part by Grants-in-aid 17590067 from the Ministry of Education, Science and Culture of Japan; by a Kitasato University Research Grant for Young Researchers and by the Uehara Memorial Foundation; and by the Kato Memorial Foundation.

REFERENCES

1. Imai, H. and Nakagawa, Y. (2003) Biological significance of phospholipid hydroperoxide glutathione peroxidase (PHGPx, GPx4) in mammalian cells. *Free Radic. Biol. Med.* **34**, 145–169
2. Imai, H., Sumi, D., Sakamoto, H., Hanamoto, A., Arai, M., Chiba, N., and Nakagawa, Y. (1996) Overexpression of phospholipid hydroperoxide glutathione peroxidase suppressed cell death due to oxidative damage in rat basophile leukemia cells (RBL-2H3). *Biochem. Biophys. Res. Commun.* **222**, 432–438
3. Imai, H., Hirao, F., Sakamoto, T., Sekine, K., Mizukura, Y., Saito, M., Kitamoto, T., Hayasaka, M., Hanaoka, K., and Nakagawa, Y. (2003) Early embryonic lethality caused by targeted disruption of the mouse PHGPx gene. *Biochem. Biophys. Res. Commun.* **305**, 278–286
4. Maiorino, M., Scapin, M., Ursini, F., Biasolo, M., Bosello, V., and Flohe, L. (2003) Distinct promoters determine alternative transcription of gpx-4 into phospholipid-hydroperoxide glutathione peroxidase variants. *J. Biol. Chem.* **278**, 34286–34290
5. Imai, H., Narashima, K., Arai, M., Sakamoto, H., Chiba, N., and Nakagawa, Y. (1998) Suppression of leukotriene formation in RBL-2H3 cells that overexpressed phospholipid hydroperoxide glutathione peroxidase. *J. Biol. Chem.* **273**, 1990–1997
6. Sakamoto, H., Imai, H., and Nakagawa Y. (2000) Involvement of phospholipid hydroperoxide glutathione peroxidase in the modulation of prostaglandin D_2 synthesis. *J. Biol. Chem.* **275**, 40028–40035
7. Sakamoto, H., Tosaki, T., and Nakagawa, Y. (2002) Overexpression of phospholipid hydroperoxide glutathione peroxidase modulates acetyl-CoA, 1-O-alkyl-2-lyso-sn-glycero-3-phosphocholine acetyltransferase activity. *J. Biol. Chem.* **277**, 50431–50438
8. Arai, M., Imai, H., Koumura, T., Yoshida, M., Emoto, K., Umeda, M., Chiba, N., and Nakagawa, Y. (1999) Mitochondrial phospholipid hydroperoxide glutathione peroxidase plays a major role in preventing oxidative injury to cells. *J. Biol. Chem.* **274**, 4924–4933
9. Nomura, K., Imai, H., Koumura, T., Arai, M., and Nakagawa, Y. (1999) Mitochondrial phospholipid hydroperoxide glutathione peroxidase suppresses apoptosis mediated by a mitochondrial death pathway. *J. Biol. Chem.* **274**, 29294–29302
10. Nakamura, T., Imai, H., Tsunashima, N., and Nakagawa, Y. (2003) Molecular cloning and functional expression of nucleolar phospholipid hydroperoxide glutathione peroxidase in mammalian cells. *Biochem. Biophys. Res. Commun.* **311**, 139–148
11. Imai, H., Suzuki, K., Ishizaka, K., Ichinose, S., Oshima, H., Okayasu, I., Emoto, K.,Umeda, M., and Nakagawa, Y. (2001) Failure of the expression of phospholipid hydroperoxide glutathione peroxidase in the spermatozoa of human infertile males. *Biol. Reprod.* **64**, 674–683
12. Brigelius-Flohe, R., Aumann, K.D., Blocker, H., Gross, G., Kiess, M., Kloppel, K.D., Maiorino, M., Roveri, A., Schuckelt, R., Ursini, F., Wingender, E., and Flohe, L. (1994) Phospholipid-hydroperoxide glutathione peroxidase. Genomic DNA, cDNA, and deduced amino acid sequence. *J. Biol.Chem.* **269**, 7342–7348
13. Kelner, M.J. and Montoya, M.A. (1998) Structural organization of the human selenium-dependent phospholipid hydroperoxide glutathione peroxidase gene (GPX4): chromosomal localization to 19p13.3. *Biochem. Biophys. Res. Commun.* **249**, 53–55
14. Borchert, A., Schnurr, K., Thiele, B.J., and Kuhn, H (1999) Cloning of the mouse phospholipid hydroperoxide glutathione peroxidase gene. *FEBS Lett.* **446**, 223–227
15. Ufer, C., Borchert, A., and Kuhn, H. (2003) Functional characterization of cis- and trans-regulatory elements involved in expression of phospholipid hydroperoxide glutathione peroxidase. *Nucleic Acid Res.* **31**,4293–4303
16. Borchert, A., Savaskan, N.E., and Kuhn, H. (2003) Regulation of expression of the phospholipid hydroperoxide/sperm nucleus glutathione peroxidase gene. Tissue-specific expression pattern and identification of functional cis- and trans-regulatory elements. *J. Biol. Chem.* **278**, 2571–2580

17. Arai, M., Imai, H., Sumi, D., Imanaka, T., Takano, T., Chiba, N., and Nakagawa, Y. (1996) Import into mitochondria of phospholipid hydroperoxide glutathione peroxidase requires a leader sequence. *Biochem. Biophys. Res. Commun.* **227** 433–439
18. Pfeifer, H., Conrad, M., Roethlein, D., Kyriakopoulos, A., Brielmeier, M., G.W. Bornkamm, G.W., and Behne, D. (2001) Identification of a specific sperm nuclei selenoenzyme necessary for protamine thiol cross-linking during sperm maturation. *FASEB J.* **15**, 1236–1238
19. Nam,S., Nakamuta, N., Kurohmaru, M., and Hayashi, Y. (1997) Cloning and sequencing of the mouse cDNA encoding a phospholipid hydroperoxide glutathione peroxidase. *Gene* **198**, 245–249
20. Pushpa-Rekha, T.R., Burdsall, A.L., Oleksa, L.M., Chisolm, G.M., and Driscoll, D.M. (1995) Rat phospholipid-hydroperoxide glutathione peroxidase. cDNA cloning and identification of multiple transcription and translation start sites. *J. Biol. Chem.* **270**, 26993–26999
21. Imai,H., Sumi, D., Hanamoto, A., Arai, M., Sugiyama, A., Kuchino, Y., and Nakagawa, Y. (1995) Molecular cloning and functional expression of a cDNA for rat phospholipid hydroperoxide glutathione peroxidase: 3′-untranslated region of the gene is necessary for functional expression. *J. Biochem.* **118**, 1061–1067
22. Roveri, A.,Casasco, A., Maiorino, M., Dalan, P., Calligaro, A., and Ursini, F. (1992) Phospholipid hydroperoxide glutathione peroxidase of rat testis. Gonadotropin dependence and immunocytochemical identification. *J. Biol. Chem.* **267**, 6142–6146
23. Maiorino, M., Wissing, J.B. Brigelius-Flohe, R., Calabrese, F., Roveri, A., Steinert, P., Ursini, F., and Flohe, L. (1998) Testosterone mediates expression of the selenoprotein PHGPx by induction of spermatogenesis and not by direct transcriptional gene activation. *FASEB J.* **12**, 1359–1370
24. Ursini, F., Heim, S., Kiess, M., Maiorino, M., Roveri, A., Wissing, J., and Flohe, L. (1999) Dual function of the selenoprotein PHGPx during sperm maturation. *Science* **285**, 1393–1396
25. Nishimura, M., Naito, S., and Yokoi, T. (2004) Tissue-specific mRNA expression profiles of human nuclear receptor subfamilies. *Drug Metab. Pharmacokinet.* **19**, 135–149
26. Matsuda, T., Nakamura, T., Nakao, K., Arai, T., Katsuki, M., Heike, T., and Yokota, T. (1999) STAT3 activation is sufficient to maintain an undifferentiated state of mouse embryonic stem cells. *EMBO J.* **18**, 4261–4269
27. Foulkes, N.S., Schlotter, F., Pevet, P., and Sassone-Corsi, P. (1993) Pituitary hormone FSH directs the CREM functional switch during spermatogenesis. *Nature* **362**, 264–267
28. De Cesare, D., Fiamia, G.M., and Sassone-Corsi, P. (2000) CREM, a master-switch of the transcriptional cascade in male germ cells. *J. Endocrinol. Invest.* **23**, 592–596
29. Don, J. and Stelzer, G. (2002) The expanding family of CREB/CREM transcription factors that are involved with spermatogenesis. *Mol. Cell. Endocrinol.* **187**, 115–124
30. Tramer, F., Vetere, A., Martinelli, M., Panfilli, F., Marsich, E., Boitani, C., Sandri, G., and Panfili, E. (2004) cAMP-response element modulator-tau activates a distinct promoter element for the expression of the phospholipid hydroperoxide/sperm nucleus glutathione peroxidase gene. *Biochem. J.* **383**, 179–185